© 2001 INIST CNRS. Tous droits de propriété intellectuelle réservés. Reproduction, représentation et diffusion interdites. Loi du 01/07/92. Articles 5, 6 et 7 des CGV.

Journal of Coastal Research	8	3	527–561	Fort Lauderdale, Florida	Summer 1992

Late Quaternary Evolution of the Northwestern Nile Delta between the Rosetta Promontory and Alexandria, Egypt

Zhongyuan Chen, Andrew G. Warne and Daniel Jean Stanley

Mediterranean Basin Program
U.S. National Museum of Natural History
Smithsonian Institution, Washington, DC 20560, U.S.A.

ABSTRACT

CHEN, Z.; WARNE, A.G., and STANLEY, D.J., 1992. Late Quaternary evolution of the northwestern Nile Delta between the Rosetta Promontory and Alexandria, Egypt. *Journal of Coastal Research*, 8(3), 527–561. Fort Lauderdale, Florida. ISSN 0749-0208.

The northwestern Nile delta of Egypt between the Rosetta promontory and Abu Qir carbonate ridge is characterized by a concave coastline backed by the Idku lagoon, extensive coastal sand flats and dunes. The late Quaternary evolution of this region is interpreted primarily on the basis of petrological and faunal analyses of 22 radiocarbon-dated cores. The subsurface study reveals thin Holocene sections in the southern and western sectors, previously unrecognized marine bay facies in the western sector, thick vegetal-rich layers of marsh origin in the eastern sector, thick barrier beach sands in the northern sector, and thick fluvial-derived sands at the Rosetta promontory. Interpretation of subsurface sediment distribution and paleogeography takes into account natural factors that determine sediment distribution (eustatic sea level, subsidence, paleoclimate and sediment transport processes) and the impact of man.

The evolving configuration of this delta area during the past ~35,000 years is shown by a series of time-slice paleogeographic maps. These maps highlight the migration of the coastline, shifts of major channel systems and shrinkage of lagoons with time. Late Pleistocene to early Holocene sequences (~35,000 to 7,500 years BP) include mostly alluvial and shallow marine siliciclastic deposits. Holocene sequences (since ~7,500 years BP) include delta-front, marine bay, lagoon, marsh and delta plain facies. Accumulation rates, highest in the sand-rich Rosetta promontory, locally exceed 600 cm/1,000 yr. The study area, in contrast to the delta region to the east, comprises open marine bay deposits and thick peats (to 5 m), and records some emergence in the area south of Abu Qir ridge.

The positions and ages of the former major Nile distributary channels in this region are revealed by analysis of radiocarbon-dated cores. These include a large Pleistocene channel which extended just to the east of Abu Qir ridge into what is now Abu Qir bay and, perhaps, further onto the Egyptian shelf. During the Holocene, the north-flowing Canopic channel was first positioned along the western margin of Idku lagoon (~6,900–4,000 yr BP), then migrated westward to just east of Abu Qir ridge (~4,000–3,000 yr BP), and then shifted eastward to its former position along the western margin of Idku lagoon (~3,000–2,500 yr BP) where it has remained until recent time. It is postulated that erosion of the Canopic promontory in presently submerged western Abu Qir bay gave rise to large volumes of sands which formed coastal ridges, broad sand flats and coastal dunes along the northwestern delta. The Bolbitic-Rosetta distributary to the east is a younger system (from ~2,500 yr BP) that, during most of its history, has been modified by man. Shallow lagoons have prevailed in the study area, at least since ~5,000 yr BP, and have been increasingly subject to human influence. Abu Qir lagoon, still in existence 200 years ago, has completely disappeared. The larger Idku lagoon is reduced to only 20% of its original size, as a function of reduced fresh water flow to the coast, land reclamation and irrigation projects. This study calls attention to the need to protect these natural habitats which are vital to man in the Nile delta.

ADDITIONAL INDEX WORDS: *Abu Qir ridge, bay facies, Canopic branch, Idku lagoon, paleogeography, Rosetta promontory, sea level change, subsidence.*

Retour catalogage le 27 AOUT 1992

INTRODUCTION

This investigation is a sedimentologic-lithostratigraphic analysis of subsurface depositional sequences of late Pleistocene to Recent age in the northwestern Nile delta, Egypt. Examination of the region between Rosetta promontory and Alexandria (Figure 1) is part of a long-term geological program, initiated at the Smithsonian Institution in 1985, to define the late Quaternary paleogeographic evolution of the entire northern Nile delta plain. Study of radiocarbon-dated sediment borings and systematic mapping of subsurface sequences are an integral part of the ongoing program to interpret changes in the Nile delta environments through time. Herein, petrologic and faunal analyses serve to define the major subsurface lithofacies and sedimentary environments in the study area, and core-to-core correlations of dated sections reveal lithofacies distributions in time and space. A series of time-slice paleogeographic maps are generated on the basis of lithofacies distributions.

Comparable investigations of the late Quaternary evolution of adjacent regions, also based

92002 received and accepted 11 January 1992.

© 2001 INIST CNRS. Tous droits de propriété intellectuelle réservés. Reproduction, représentation et diffusion interdites. Loi du 01/07/92. Articles 5, 6 et 7 des CGV.

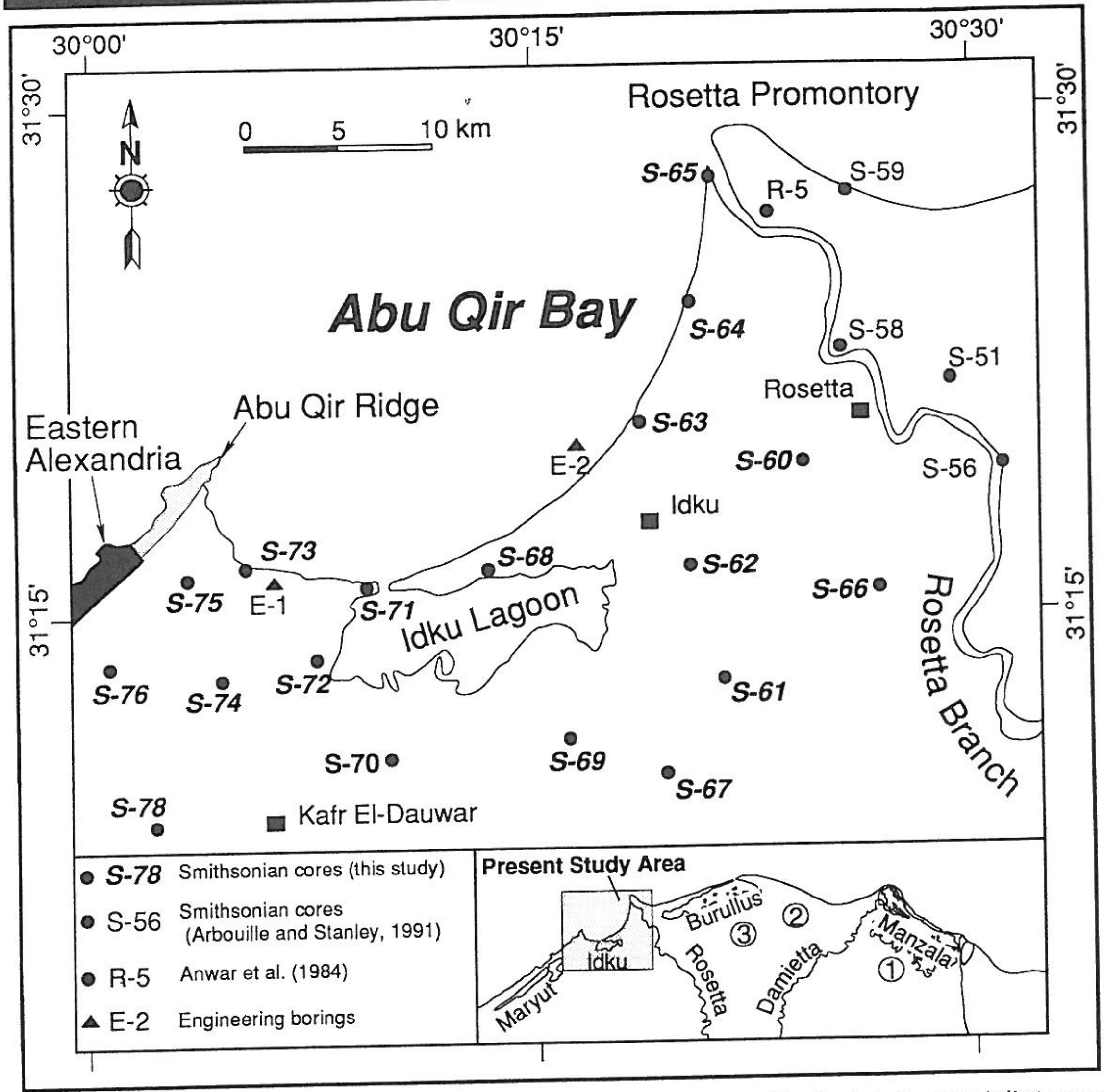

Figure 1. Map of the northwestern Nile delta area showing location of sediment cores used in this study. Inset map indicates areas to the east of the study area which were previously cored and studied as part of the Smithsonian's Nile Delta Project: (1) Coutellier and Stanley, 1987; (2) Stanley *et al.*, 1992; and (3) Arbouille and Stanley, 1991.

largely on analysis of radiocarbon-dated sediment cores, have been carried out to the east (COUTELLIER and STANLEY, 1987; ARBOUILLE and STANLEY, 1991; STANLEY *et al.*, 1992). These companion studies (Figure 1, inset) have demonstrated that, as in the case of most of the world's deltas (BROUSSARD, 1975; COLEMAN, 1982), modifications of the Nile delta with time have been induced by eustatic sea level and climatic oscillations, subsidence (compaction, isostatic depression, neotectonics) and sediment transport processes. Previous studies have shown that, in addition to interplay of these natural phenomena, the Nile delta is currently undergoing marked physiographic and ecologic changes as a result of human activity. These latter changes include land reclamation, agricultural, aquacultural, irrigation and industrial projects (BUTZER, 1976; WATERBURY, 1979).

The Nile delta is unusual among the large deltas

© 2001 INIST CNRS. Tous droits de propriété intellectuelle réservés. Reproduction, représentation et diffusion interdites. Loi du 01/07/92. Articles 5, 6 et 7 des CGV.

of the world in that it has formed along a microtidal coastline in an arid setting. This fan-shaped, wave-dominated deltaic complex is the largest depocenter in the Mediterranean Sea. Earlier geomorphological and geological studies of the area between Rosetta promontory and Alexandria include those by FOURTAU (1896), TOUSSOUN (1922, 1934), ATTIA (1954), EL-FAYOUMY *et al.* (1975), WEIR *et al.* (1975), ZAGHLOUL *et al.* (1977), RIZZINI *et al.* (1978), UNDP/UNESCO (1976, 1978), SAID (1981), ABDEL-KADER (1982), ANWAR *et al.* (1984), EL ASKARY and FRIHY (1986), EL FATTAH and FRIHY (1988), EMERY *et al.* (1988), FRIHY *et al.* (1988), SMITH and ABDEL-KADER (1988), SESTINI (1989), FRIHY and KOMAR (1991), BLODGET *et al.* (1991), NAFAS *et al.* (1991) and STANLEY and CHEN (1991). To date, however, there has been no systematic sedimentologic and stratigraphic study of subsurface sequences, or detailed paleogeographic analysis of the northwestern delta.

Earlier studies have indicated that it is difficult to distinguish distinct facies within sandy sections using standard petrological techniques (FRIHY and STANLEY, 1988). Petrographical study coupled with faunal analyses provides a means to discriminate among various sand facies. Discrimination of different sand facies in this study allows better determination of depositional environments and, thus, more precise interpretation of paleogeography. Better definition of sand facies also helps delineate former Nile distributary channels, barrier beaches and sand flats.

One of the major goals of the present investigation is to help predict changes in the configuration of this Nile delta sector. Interpretation of radiocarbon-dated cores enables us to evaluate the relative importance of natural and human-induced factors that affect delta evolution through time. Such analysis is essential in devising effective plans to help protect this low-lying coastal region.

METHODOLOGY

The twenty-two Smithsonian sediment cores used in this study were collected in the northwestern Nile delta, Egypt, during two field expeditions in 1989 and 1990 (Figure 1). These 7.5 cm diameter cores, recovered using a trailer-mounted rotary percussion (Acker-2) drilling rig, range in length from 19 to 46 m and are spaced ~6 to 12 km apart. Cores were collected as continuous sections where sediment was cohesive, and as washings (by circulating water) where sandy and noncohesive. Eighteen of these cores (S-60 to S-76, S-78) were analyzed during the course of this study (Figure 1); the other four cores (S-51, S-56, S-58, S-59) were examined in a previous investigation (ARBOUILLE and STANLEY, 1991). Lithologic logs of two engineering borings (E-1, E-2) and one published log (R-5, ANWAR *et al.*, 1984) were incorporated into the subsurface data base. Moreover, lithologic logs published by ATTIA (1954), UNDP/UNESCO (1978) and SESTINI (1989) were consulted.

All cores were split and X-radiographed to better define sedimentary structures and traces of plants and organisms. Color, hardness, stratal boundaries, sedimentary structures, fossil content, root traces and other microscopic features were recorded for each core (*cf.* method of COUTELLIER and STANLEY, 1987). From the twenty-two cores, 571 samples were collected for petrographic analysis at each lithological boundary, or at less than 1 m intervals in thick homogeneous sections. An additional 52 samples were radiocarbon dated (using total organic matter, plants and/or shell), of which 42 provided viable ages to establish a chronostratigraphic framework.

Size analysis of the 571 petrologic samples involved determination of clay (<2 μm), silt (2–63 μm) and sand (>63 μm) fractions. In addition average sand size (very fine, fine, medium, coarse, very coarse) were determined for 283 samples from sand fractions and washings in the twenty-two cores of this study. This was done by comparing these samples (under a reflected light microscope) to grain-size standards in a Grain Sizing Folder (©Forestry Suppliers Inc.). Sand size analysis proved to be particularly useful for differentiating river channel sands, nearshore/beach sands and lagoon/coastal sands.

Petrographic analysis (*cf.* method of COUTELLIER and STANLEY, 1987) of the sand-size fraction in mud sections was used to distinguish the major clay-rich facies. Relative percentages of 17 sand-size components were calculated from point counts of >300 grains for all of the samples (method of FRIHY and STANLEY, 1988). Counted components include: 8 mineralogical (light and heavy mineral, mica, glauconite/verdine, pyrite, gypsum, lithic fragment, aggregate); 6 faunal (indeterminate shell fragments, foraminifera, ostracod, gastropod, pelecypod and sponge); and 3 floral (diatom, plant fragment and seed). This method is particularly useful for distinguishing among marine bay, del-

© 2001 INIST CNRS. Tous droits de propriété intellectuelle réservés. Reproduction, représentation et diffusion interdites. Loi du 01/07/92. Articles 5, 6 et 7 des CGV.

Table 1. *Relative percentages, from two separate analyses, of partially stained grains and of compositional components for 19 representative samples: 1 near-surface sample from a kôm (southwest of Idku lagoon) and 18 subsurface samples from 11 Smithsonian cores recovered in the study area (Figure 1). The complete petrographic data set is compiled in a comprehensive data-base available at the U.S. National Museum of Natural History (MEDIBA, 1992).*

Facies		Sample No.	Depth (m)	Grain Size*	Part. Stain %	Light Mins. %	Heavy Mins. %	Mica %	Verdine Glauconite %	Pyrite %	Gypsum %	Lithic Frags. %	Aggregates %	Plant Debris %	Plant Seeds %	Forams %	Shell Frags %	Ostracods %	Sponge Spicules %	Diatoms %	Unident. Carbon. Particles %
Holocene																					
Fluvial	Kom	90-1	0.20	F	41.1	91.2	4.0				0.6		4.0								0.3
	Silt Plain	S72-18	3.51	S		86.0	3.4	6.2	1.6		0.3		1.2		0.3		0.9				
	Sand Flat	S64-2	0.50	F	62.1	88.4	9.4	0.3			1.6						0.3				
	Channel	S71-7	6.90	F	33.9	83.4	13.8	1.9	0.3		0.3				0.3						
Coastal wetland	Fresh Marsh (Peat)	S66-13	14.00	S		4.3				0.7				92.4	0.7		1.3		0.7		
	Brackish Muds	S68-35	6.56	S		39.4		1.3		6.3			1.6	20.3		5.9	24.7	0.6			
	Fluvially Influenced	S73-36	5.03	S		65.3	1.0	13.1	0.7	0.3	1.3		1.3	16.1		0.3	0.7				
	Wash-over	S68-9	7.93	F-M	8.0	90.9	4.9	0.3	2.3	0.7						0.3	0.7				
	Lagoon Muds	S72-7	6.10	S		29.3	5.5	21.2	28.6					11.3		0.6	0.3	0.6	1.3	1.3	
Coastal	Beach	S65-20	28.30	F-M	31.5	54.7	42.2		0.6	0.9						0.6	0.6				0.3
	Nearshore	S63-11	14.30	F	15.9	81.4	10.6	0.6	3.2		1.6					1.0	1.6				
	River Mouth	S65-33	47.80	F	44.6	75.0	19.6	3.2	0.3		0.6			0.6		0.3	0.3				
Marine Bay		S75-29	13.42	S-VF		60.0	5.5	0.7			1.0			0.3		29.4	2.3	0.6		0.3	
Delta-front		S64-15	18.80	S-F	16.7	60.9	9.0	7.6	12.2	1.0				2.0		2.2	1.7		0.7		2.7
Late Pleistocene to Early Holocene																					
Transgressive sands		S64-19	23.70	F-C	16.1	93.7	5.3				0.3					0.3	0.3				
Late Pleistocene																					
Flood Plain Stiff Muds		S69-19	10.82	S		92.3	2.0	0.6			2.9			2.3							
Drowned Flood Plain		S71-31	40.41	F	26.3	88.6	5.4	0.3			0.6	3.2				0.3					1.6
Drowned Channel		S73-22	29.74	F-C	35.8	84.8	6.8									6.8	1.3	0.3			
Alluvial		S67-9	12.35	F-M	36.5	91.1	7.3	0.3	1.3												

* S—Silt; VF—Very Fine sand; F—Fine sand; M—Medium sand; C—coarse sand

© 2001 INIST-CNRS. Tous droits de propriété intellectuelle réservés. Reproduction, représentation et diffusion interdites. Loi du 01/07/92. Articles 5, 6 et 7 des CGV.

ta-front, marsh, lagoon and silt-plain facies (Table 1).

Combined compositional and stained-grain analysis (*cf.* method of STANLEY and CHEN, 1991) was used to differentiate several previously unrecognized Nile delta sand facies. Relative percentages of the dominant sand-size components were determined from the original counts of >300 grains per sample. In addition, the relative percentages of iron-stained, partially stained and unstained quartz grains were obtained from additional counts of >300 grains per sample. This analysis was performed on 9 samples from a thick all-sand core (S-65), 12 samples from 7 other cores, and also 7 surficial samples from the modern nearshore, beach and kôm (low silt and sand hills); the data from selected samples are listed in Table 1. Having characterized the various sand facies in the 8 cores and 3 modern environments, it was then possible to distinguish and correlate comparable facies in the other cores in the study area. This method proved most useful for distinguishing among river channel, river mouth, nearshore marine/beach, lagoon/beach, and sand flat/dune facies.

Molluscan fossil communities have been shown to be representative of specific range of marine conditions and water depths (DI GERONIMO and ROBBA, 1976; BERNASCONI *et al.*, 1991). In this study, molluscan paleocommunity analysis was performed (M.P. BERNASCONI, *written communication*, 1991) on 13 samples from two cores (S-73 and S-75). Paleocommunity analysis contributed to differentiation of a previously unrecognized marine bay facies.

On the basis of the above analyses, the various late Quaternary lithofacies were distinguished for each core. Core-to-core correlations were then established, taking into account available radiocarbon ages. Correlations brought about more refined interpretation of lithofacies distribution (and associated environments of deposition) in time and space. A series of time-slice paleogeographic maps, based primarily on the facies distribution, was then compiled. All relevant information is included in MEDIBA (1992).

A generalized geomorphic-land use map (Figure 2) of the northwestern Nile delta was compiled to better interpret present-day sedimentary environments in terms of subrecent to modern coastal and fluvial processes. This map was compiled primarily from Landsat-5 Satellite Thematic Mapper images (bands 3, 4, 5, 7) which were taken during a survey in December, 1986, and published by IWACO (1989). Additional information was obtained from topographic maps (scale 1:50,000) prepared by U.S. DEFENSE MAPPING AGENCY (1977, 1981), and other pertinent maps (ARROWSMITH, 1802, 1807; EL FISHAWI and EL ASKARY, 1981; FRIHY, 1988; FRIHY *et al.*, 1988).

DESCRIPTION OF THE STUDY AREA

The study area, ~60 km from east to west and extending 25–30 km south of the coast, comprises a series of distinct geomorphic areas: Rosetta promontory, Abu Qir ridge, beach, backshore sand flat, strand plain, backshore depression, coastal dune, lagoon, distributary channel, kôm (low hill), drain and canal, and arable land to the south (Figure 2). The coastline between the Rosetta promontory to the east and Abu Qir ridge to the west is concave seaward in outline. Rosetta promontory extends ~14 km northwestward, and Abu Qir carbonate ridge protrudes ~5 km northeastward into the Mediterranean Sea. The Rosetta branch is one of the two active distributaries of the River Nile that flow across the delta. Closure of Aswan Dam in 1964 and irrigation projects in the delta have reduced sediment supply to the coast to essentially zero; in consequence, the Rosetta promontory has undergone substantial erosion. In addition to the coastline, other distinctive geomorphic features in the study area include: Idku lagoon, the third largest of the Nile delta brackish water bodies; coastal dune fields along the western margin of the Rosetta promontory; broad sand flats west of the Rosetta promontory; and kôms south of Idku lagoon (Figure 2).

Coastal Area

The Rosetta to Abu Qir coast includes the Rosetta promontory, beach, backshore sand flat, strand plain, backshore depression, coastal dune, and Abu Qir ridge (EL-FAYOUMY *et al.*, 1975; EL FISHAWI and EL ASKARY, 1981; FRIHY *et al.*, 1988). The width of the coast, including the above environments, is highly variable, ranging from 0.5 km near the Abu Qir ridge to 10 km immediately west of the Rosetta branch (Figure 2).

The Rosetta promontory, a triangular-shaped landform which currently extends ~14 km north-northwestward into the sea, is the most distinctive geomorphic feature in the study area. A series of studies show that it is undergoing rapid erosion by marine waves and currents, resulting in rapid

© 2001 INIST CNRS. Tous droits de propriété intellectuelle réservés. Reproduction, représentation et diffusion interdites. Loi du 01/07/92. Articles 5, 6 et 7 des CGV.

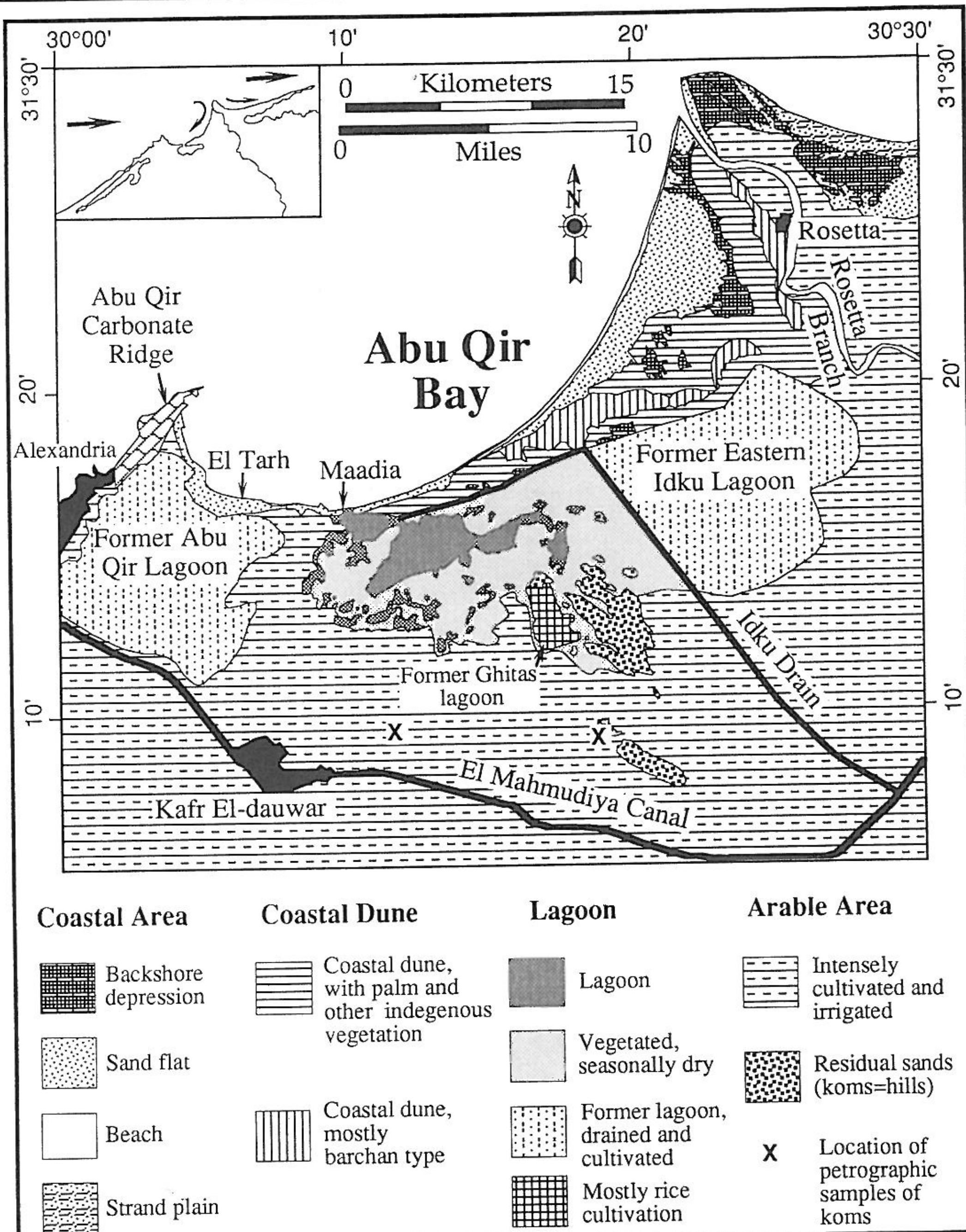

Figure 2. Geomorphic-land use map of the delta plain study area. Primary information source for this map is Landsat-5 satellite Thematic mapper images taken in a December 1986 survey (IWACO, 1989). The Rosetta promontory and Abu Qir ridge form the boundaries of the arcuate shoreline south of Abu Qir Bay. Descriptions of the various geomorphic features are presented in text. Inset map shows prevaling wind (heavy arrow) and littoral current directions (smaller arrows) in the region.

© 2001 INIST CNRS. Tous droits de propriété intellectuelle réservés. Reproduction, représentation et diffusion interdites. Loi du 01/07/92. Articles 5, 6 et 7 des CGV.

retrogradation (up to 100 m/yr) of the headland (FRIHY, 1988; BLODGET *et al.*, 1991), and concentration of opaque heavy minerals (black sands; see Figure 3A and B) as a result of winnowing (RITTMANN and NAKHLA, 1958). Marine and eolian transport of large volumes of eroded sediment to each side of the Rosetta promontory has resulted in increased rapid accretion and progradation of adjacent beaches and backshore sand flats (Figure 2).

Beaches and backshore sand flats consist primarily of very fine to medium quartz sands; micas, heavy minerals (generally opaque), pebbles, and mollusc shells are common in some places, locally abundant. Carbonate sands and pebbles increase in frequency toward Abu Qir ridge (EL-FAYOUMY *et al.*, 1975; STANLEY and HAMZA, 1992) and further west, toward the carbonate province west of the delta (EL-WAKEEL and EL-SAYED, 1978; SUMMERHAYS *et al.*, 1978). Backshore sand flats occupy ~55 km², and extend to as much as 6 km inland along the northwestern flank of the Rosetta promontory. Beaches and backshore flats are generally <1.0 m above sea level, but interspersed dunes reach 2 m in elevation (EL-FAYOUMY *et al.*, 1975).

The strand plain, composed of accreted beach ridges which mark the position of former shorelines, has developed mainly along the east coast of the Rosetta promontory (Figures 2 and 3B). This plain covers an area of ~10 km², is partially covered by coastal dunes, and is currently prograding eastward (partially seaward). The strand plain developed by longshore currents and winds which transported large volumes of sand derived from the rapidly eroding Rosetta promontory.

There are several depressions landward of beach ridges, backshore sand flats, and strand plains (Figure 2). These shallow backshore depressions, which are generally below sea level (to −1.0 m), are periodically inundated by marine water, particularly during winter storm season. These depressions form by longshore transport of sand, where subsequent formation of spits and beach ridges separate these topographic lows from the sea.

Coastal dunes are distributed along the northern coastline to the west and south of the Rosetta promontory (Figure 3C). They occupy ~40 km², range in height from 2 to 16 m, and are generally 1–3 km wide. Many of these dunes are of the barchan type, and these are generally oriented northeast-southwest with their leeward side facing southeast (FRIHY *et al.*, 1988). It is of note that hand-dug pits in interdune lows (generally 2 to 4 m in elevation) fill with ground water, indicating that the water table is high in this region. Coastal dunes, derived primarily from nearshore sands, are moved southeastward by winds from the northwest (Figure 3D); eolian sand is stabilized by palms and other indigenous vegetation (Figure 2). The overall configuration of coastal dune fields on the west side of the Rosetta promontory and northeastern Idku lagoon conform with prevailing wind measurements. Observation of individual dune migration indicates that these features are expanding to the east and southeast (EL FISHAWI and EL ASKARY, 1981) and are encroaching onto cultivated areas.

Abu Qir ridge extends as a distinct feature from Abu Qir Bay and Alexandria westward to Arab's Bay (BUTZER, 1960). Alexandria is built on this SW-NE trending carbonate ridge of Late Pleistocene age. Its elevation decreases from 25 m in the west to 6 m near Abu Qir. To the west of the study area, the ridge is quarried for building and industrial use. STANLEY and HAMZA (1992) determined that limestones forming the ridge are primarily bioclastic and oolitic grainstones deposited under shallow marine conditions. Interbedded paleosols in this ridge indicate intermittent subaerial exposure. Bathymetric maps of Abu Qir Bay (UNDP/UNESCO, 1978) reveal that a portion of this ridge extends below sea level to the northeast from ~4 km of the present shoreline. Ruins on the submerged ridge are believed to be remains of the ancient Hellenistic city of Canopus (or Kanopis), which is reported to have been occupied (and above sea level) as recently as 2,000 years ago (TOUSSOUN, 1934). These ruins are presently as deep as 5 m below sea level.

Lagoons

Idku, the third largest Nile delta lagoon, is located immediately south of Abu Qir Bay (Figure 2). The lagoon currently occupies ~120 km², with water depths ranging from 0.5 to 1.5 m and salinities from 0.5 to 18 parts per thousand (KERAMBRUN, 1986). The eastern part of the Idku lagoon, drained by man and now intensely cultivated, can still be recognized on satellite images (Figure 2). The lagoon bottom is sandy and contains abundant plant debris in the vicinity of the present outlet to the sea, near Maadia (Figure 3E); elsewhere, the lagoon bottom is muddy and contains

© 2001 INIST CNRS. Tous droits de propriété intellectuelle réservés. Reproduction, représentation et diffusion interdites. Loi du 01/07/92. Articles 5, 6 et 7 des CGV.

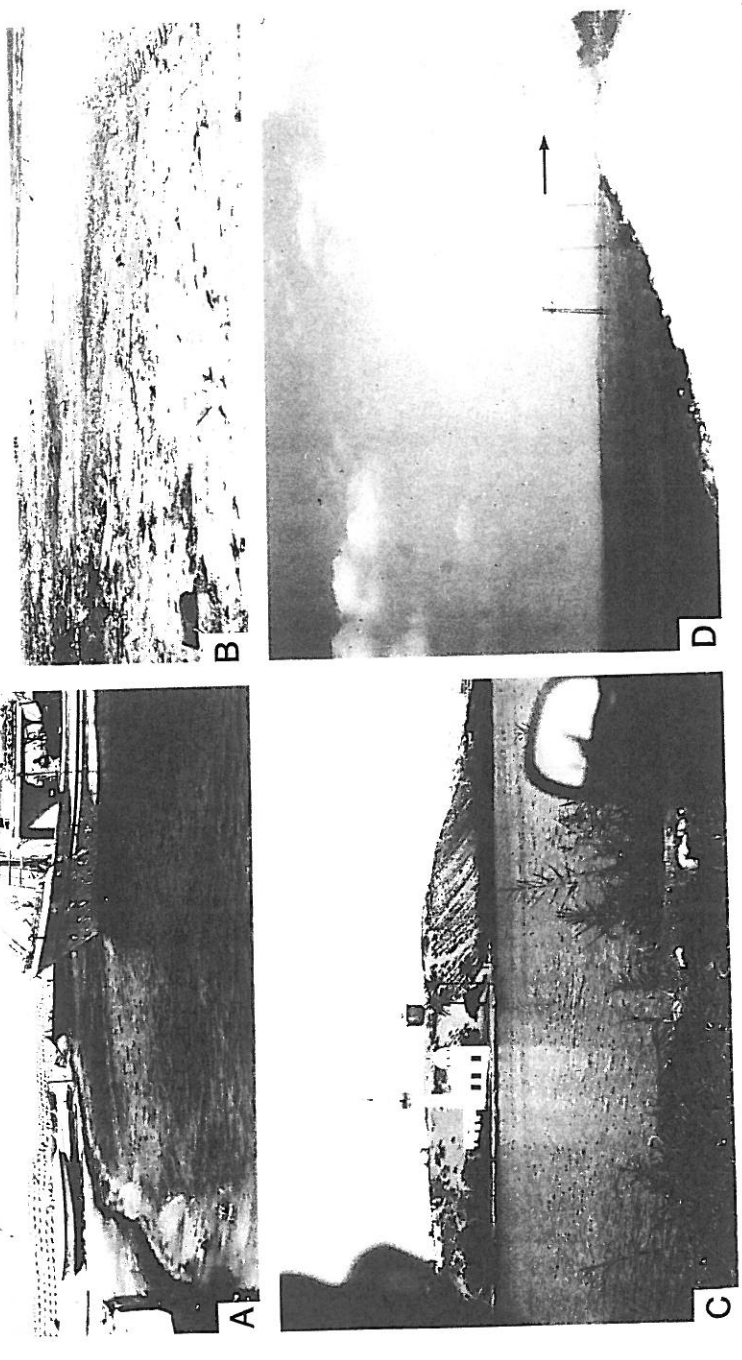

Figure 3. Photographs of selected geomorphologic and sedimentological features in the study area (A) mouth of the Rosetta promontory, showing black sands (heavy minerals) concentrated by wave current winnowing; recent (1989) sea wall along the west channel margin in shown in background. (B) broad strand plain on the eastern margin of the Rosetta promontory (near boring site S-59). (C) Coastal sand and dune field south of the town of Rosetta forming the west bank of the Rosetta distributary. (D) Sand storm, with sediment moved landward (arrow) by southeast-directed wind, over the eastern margin of Rosetta promontory. (E)

© 2001 INIST CNRS. Tous droits de propriété intellectuelle réservés. Reproduction, représentation et diffusion interdites. Loi du 01/07/92. Articles 5, 6 et 7 des CGV.

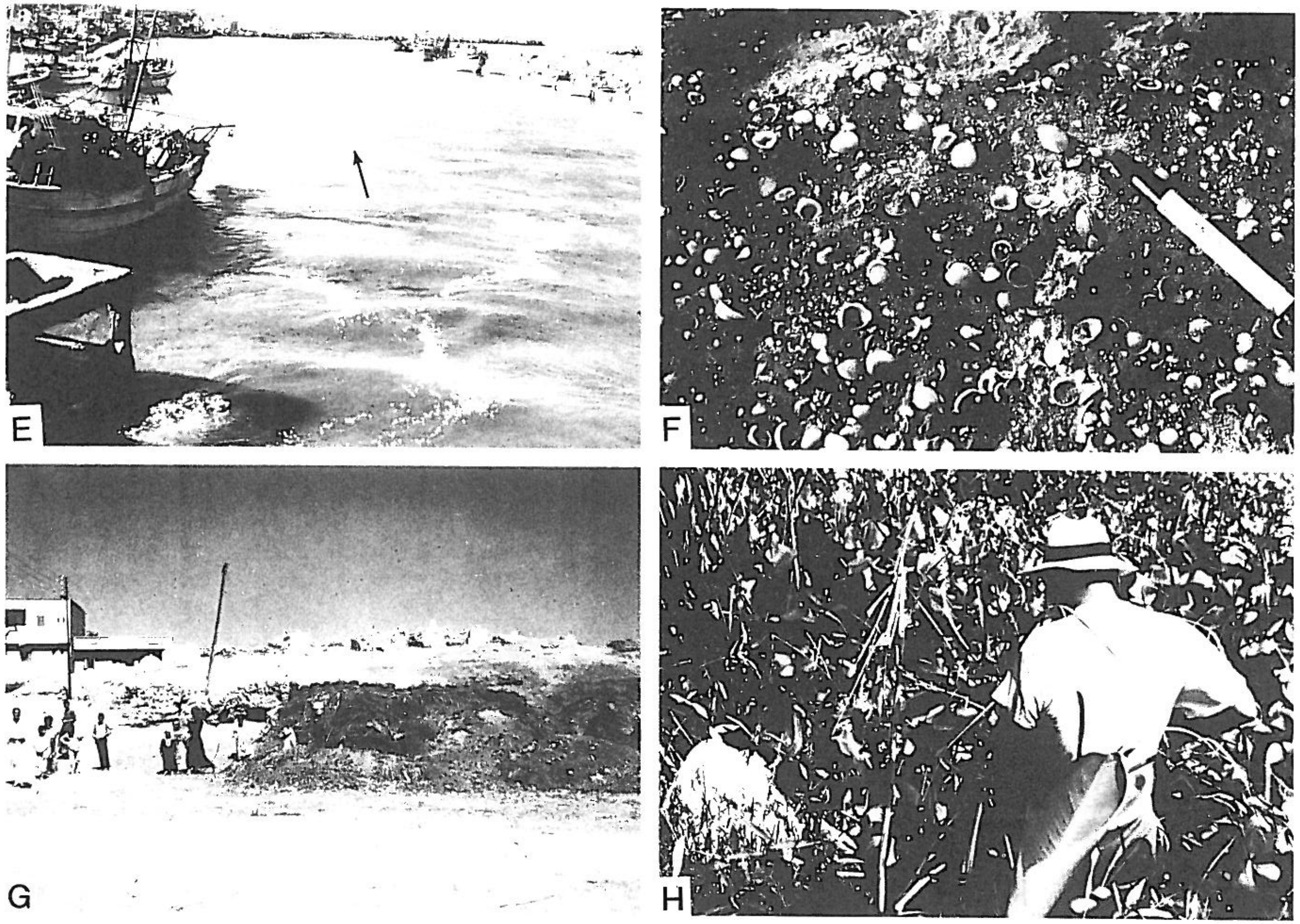

Outlet of Idku lagoon at Maadia; note powerful outflow current (arrow) toward the Mediterranean. (F) Mollusc shells concentrated on the former floor of Abu Qir lagoon, which is now a drained, cultivated region (near boring site S-75). Marker pencil is 15 cm long. (G) Kôm at El Nakhla el Bahairya formed of fine sand and silt (about 3 km southeast of boring S-67); note that this hill, as most such features in the northern, low-lying delta, serves as a cemetery. (H) Channel of the Nile's Rosetta branch near Mutubis, no longer subject to annual flooding, is now locally silted and choked with water hyacinth.

© 2001 INIST CNRS. Tous droits de propriété intellectuelle réservés. Reproduction, représentation et diffusion interdites. Loi du 01/07/92. Articles 5, 6 et 7 des CGV.

abundant mollusc shells (SAAD and EZZAT, 1972). The irregular southern lagoon margin is covered with dense hydrophetic plants. Numerous small islands (too small to show in Figures 1 and 2) dot the lagoon surface and vary in number and size according to the season (U.S. DEFENSE MAPPING AGENCY, 1977; UNDP/UNESCO, 1978). Various species of *Tilapia, Mugil* and *Anguilla* are abundantly fished from this water body (KERAMBRUN, 1986), although productivity has declined since closure of the Aswan Dam in 1964. The lagoon is polluted and mercury, for example, is present at concentrated levels (EL SOKKARY and MULLER, 1989).

Former Lake Ghitâs, a southern extension of Idku lagoon (U.S. DEFENSE MAPPING AGENCY, 1977), has been altered by man and is now used for agriculture and aquaculture (Figure 2). Abu Qir lagoon (Figure 3F), once located east of Alexandria and south of Abu Qir city (Figure 2), was a wetland area until at least the early nineteenth century (ARROWSMITH, 1802, 1807). Although now completely drained and cultivated, its trace can still be distinguished on satellite images.

Canals and Drains, Kôms, and Arable Lands

An extensive network of irrigation canals and drains covers most of the study area (U.S. DEFENSE MAPPING AGENCY, 1977). El Mahmudiya canal and Idku drain are the two principal waterways in the study area (Figure 2). The present investigation reveals that El Mahmudiya canal follows part of the course of the former Canopic channel, once a major distributary of River Nile (*cf.* TOUSSOUN, 1922; SAID, 1981).

Several conspicuous hills, referred to as kôms, rise to as much as 6 m above the otherwise flat delta plain south of Idku lagoon (Figure 2). These hills (most are NW-oriented) are largely composed of fine and medium sand and silt. Many have been altered by cultivation or are used as cemeteries (Fig. 3G); most can still be identified on aerial photographs and satellite images.

A large portion of the arable land in the study area is less than 1 m above sea level (UNDP/UNESCO, 1978; TITUS, 1986; SESTINI, 1989), and is part of the fertile Nile crescent in which nutrient-rich silts and muds were, until recently, supplied by annual floods. Continued sea level rise and lack of sediment input make this area vulnerable to increased salinization of the groundwater or even inundation by the sea.

Depositional Processes Affecting the Northwestern Nile Delta

The geomorphic evolution of the Nile delta between Rosetta promontory and Alexandria has been largely controlled by Nile littoral hydrodynamics. This microtidal coast has diurnal tides averaging 0.3 m along the northwestern Nile delta. The average wave height in the Abu Qir Bay region is between 0.5 and 1.0 m, whereas maximum wave height is seasonal, ranging from 2.5 m in summer to 4.0 m in winter (NAFAS *et al.*, 1991). Average wave period is between 7 and 8 sec. (NAFAS *et al.*, 1991).

Dominant wind is to the southeast (QUELENNEC, 1977), and wave approach is from the west and northwest, driving coastal currents to the east (INMAN and JENKINS, 1984). Seaward of the breaker zone, currents flow to the east at an average velocity of 15–20 cm/sec (COLEMAN *et al.*, 1981), and are transporting large volumes of sediment (SUMMERHAYES *et al.*, 1978; COLEMAN *et al.*, 1981). These eastward-directed littoral currents are deflected by the Rosetta promontory, resulting in a counter-clockwise eddy current (UNDP/UNESCO, 1977) in Abu Qir Bay (Figure 2, inset map). Until the recent emplacement of coastal protection structures, these currents rapidly eroded the Rosetta headland, transporting sediments toward the rapidly accreting beaches and sand flats along the two flanks of the promontory (UNDP/UNESCO, 1977; SESTINI 1989).

The Abu Qir coastal region can be subdivided into two distinct sectors (ABDEL-KADER, 1982) on the basis of shoreline configuration and nearshore bathymetry: Rosetta-Maadia and Maadia-Abu Qir ridge stretches (Figure 2). The Rosetta-Maadia sector is smooth; seaward, the bathymetric contours also record an even and gentle gradient. In contrast, the Maadia-Abu Qir ridge coastline is irregular, and the bathymetric contours seaward of this sector record an uneven seafloor. Differences in the configuration and bathymetry of these two sectors are related to littoral current processes. The smooth coastline between Rosetta and Maadia is the result of erosion of Rosetta promontory sands and subsequent southwest littoral transport and accretion along its western flank. In contrast, the irregular coastline between Maadia and Abu Qir ridge is protected from the eastward-directed littoral currents by the Abu Qir ridge promontory; thus, this sector receives little sediment transport by longshore current with which to develop a smooth, accretionary coastline.

© 2001 INIST CNRS. Tous droits de propriété intellectuelle réservés. Reproduction, représentation et diffusion interdites. Loi du 01/07/92. Articles 5, 6 et 7 des CGV.

At present, River Nile discharge and sediment transport to the coast by way of the Rosetta promontory is negligible (UNDP/UNESCO, 1978). Salt water, entering the mouth of the Rosetta, extends upchannel about 25 km to the Nile barrage at Mutubis (Figure 3H). Prior to closure of the Aswan High Dam in 1964, the annual River Nile discharge was ~18 to 55 × 10^9 m^3/yr, in which floods delivered an average 34 × 10^9 m^3/yr to the coast (EL DIN, 1977; HASSAN, 1981; COLEMAN, 1982). Prior to 1964, the suspended load was estimated to exceed 111 × 10^9 kg/yr, and 93–98% of this sediment was delivered to the coast during July-November flood periods (HOLEMAN, 1968; EL DIN, 1977). Sediment load during floods was composed of 25% sand, 45% silt and 30% clay in the northern delta (EL DIN, 1977). Most of the sediment was derived from the Ethiopian Highlands which is drained by the Blue Nile and Atbara rivers (SHUKRI, 1950; HASSAN, 1981). The present Rosetta channel is locally silted and partially filled with plants such as water hyacinth and phragmites (Figure 3H).

Fluvial and climatic conditions affecting the Nile delta region and adjacent Mediterranean have varied during the Holocene (BELL, 1970; WENDORF *et al.*, 1976; STANLEY, 1978; RIEHL and MEITIN, 1979; HASSAN, 1981; PETIT-MAIRE, 1989). The general wind, current and wave, as well a pre-Aswan (1964) river discharge conditions discussed above are considered to be representative of Nile delta plain and coastal conditions during much of the mid- to late Holocene.

DESCRIPTION AND INTERPRETATION OF LATE QUATERNARY FACIES

Subsurface lithofacies in the Nile delta were initially distinguished and interpreted by macroscopic observations of split core sections and by petrographic analyses of core samples (*cf.* COUTELLIER and STANLEY, 1987). Interpretation of depositional environments associated with these facies was enhanced by combined compositional and stained grain (*cf.* STANLEY and CHEN, 1991) and molluscan paleocommunity (*cf.* BERNASCONI *et al.*, 1991) analyses.

Lithofacies are described below, from oldest to youngest. A general synthesis of vertical and lateral facies relationships is presented in Figure 4. Most of these lithofacies have been described in previous Nile delta investigations to the east (COUTELLIER and STANLEY, 1987; ARBOUILLE and STANLEY, 1991; STANLEY *et al.*, 1992). In addition to these, six new Nile delta facies are recognized: Late Pleistocene drowned channel sands, and drowned flood-plain sands and muds; Holocene marine bay muds, sand flat, silt plain and river mouth sands. These newly-described facies are distinguished from previously defined facies primarily on the basis of compositional and stained grain analysis (*cf.* STANLEY and CHEN, 1991).

Late Pleistocene Sediment Types

Late Pleistocene core sections, radiocarbon dated at more than 10,000 years before present (BP), consist of tan to brown sands and green to brown stiff muds which represent several distinct environments of deposition. Previous clay mineralogical studies in the eastern Nile delta show that somewhat higher proportions of smectite occur in the late Pleistocene than in the overlying Holocene section; this is believed to indicate that late Pleistocene sediments, for the most part, accumulated in fluvial-terrestrial rather than marine environments (ABU-ZEID and STANLEY, 1990; ABDEL WAHAB and STANLEY, 1991).

Alluvial to Shallow Marine Sands

Yellowish brown (10YR 5/4) to light olive gray (5Y 5/2) to olive gray (10Y 5/2), very fine- to coarse-grained, rather poorly sorted sands are present in the lower proportions of most cores in the southern part of the study area. These sands are primarily composed of iron-stained quartz (Table 1); common accessory components include feldspar, mica, lithic fragments, heavy minerals and shell fragments. Core sections of this facies as long as 25 m have been recovered during Smithsonian drilling expeditions (MEDIBA, 1992); several well records reported by ATTIA (1954) indicate that this facies may locally exceed 50 m in thickness. Very small amounts of calcium carbonate (few small broken shell fragments) preclude direct radiocarbon dating; however, the stratigraphic position of these sands between, or below, dated stiff mud intervals indicates a period of accumulation from ~35,000 (in S-69) to 11,000 years BP (in S-73). Fauna is rather sparse, although gastropods and ostracods are locally present. These sands are interpreted to be mostly alluvial deposits with some shallow marine or lagoon influence. Composition of sands indicates a derivation from East African highlands (*cf.* SHUKRI, 1950; FOUCAULT and STANLEY, 1989).

© 2001 INIST CNRS. Tous droits de propriété intellectuelle réservés. Reproduction, représentation et diffusion interdites. Loi du 01/07/92. Articles 5, 6 et 7 des CGV.

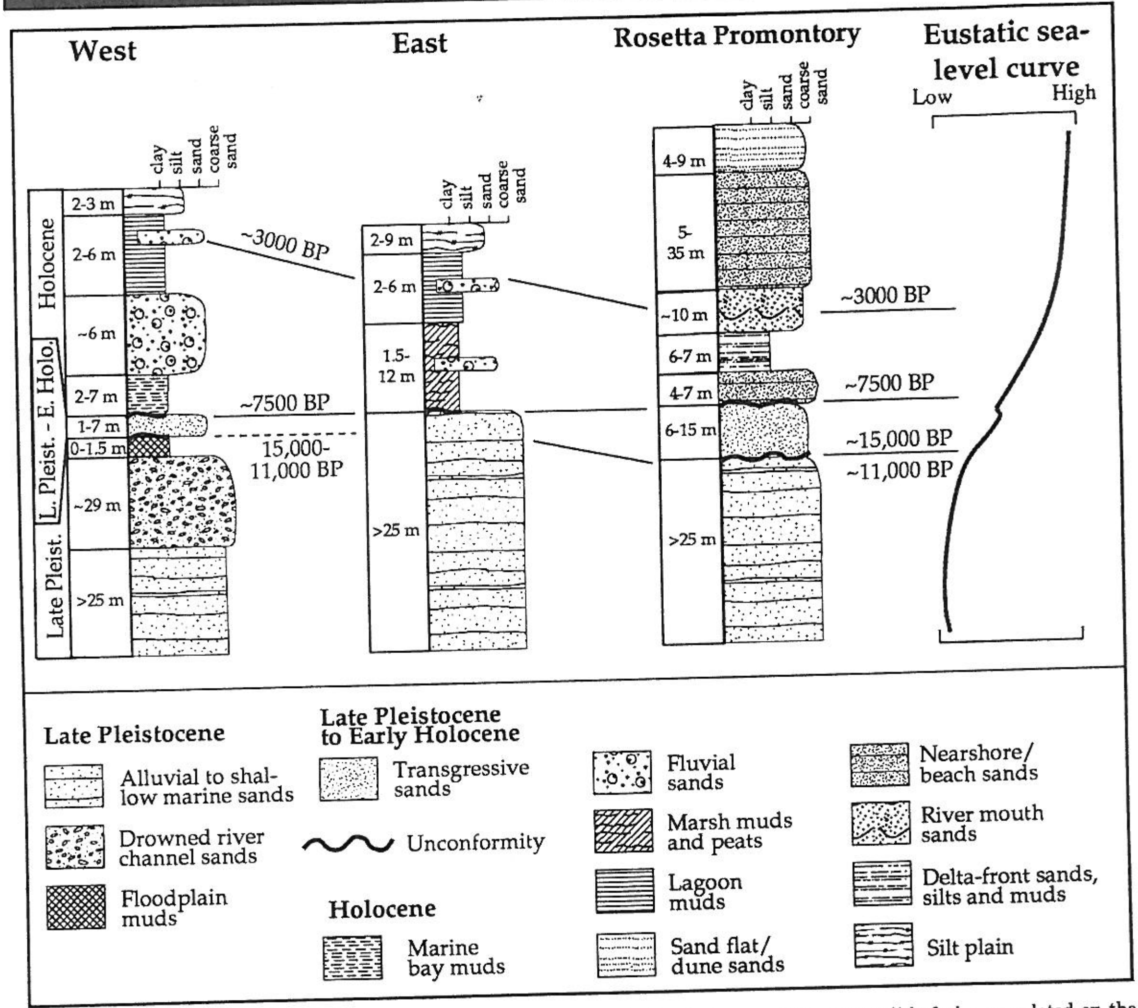

Figure 4. Generalized lithostratigraphic sections from three regions in the study area. The various lithofacies, correlated on the basis of radiometric dates are related to eustatic sea level changes during the late Pleistocene and Holocene (generalized sea level curve, on right, after Lighty *et al.*, 1982; Fairbanks, 1989).

Drowned Channel Sands

Light brown (5YR 5/6) to moderate yellowish brown (10YR 5/4), coarse- to very coarse-grained, poorly sorted sands occur in the lower portion of core S-73. Although the general composition of these sands is comparable to alluvial sands described above, drowned channel sands contain 30–50% very coarse, rounded and highly stained quartz grains, and 1–7% foraminifera (Table 1). A 29 m thick section of these sands was recovered in core S-73. A radiocarbon date from the stiff muds at top of the sands indicates that the facies was deposited before 11,000 years BP. The sphericity of the grains suggests that these sands were transported for a considerable distance, perhaps from the upper Nile region, and they are interpreted to have been deposited in a major river channel in proximity to the coast. Of note is the presence of glauconite and shell fragments suggesting that this paleochannel was periodically influenced by lagoons or the sea (*cf.* CHEN and YANG, 1991).

Drowned Flood Plain Sands and Stiff Muds

Moderate yellowish brown (10YR 5/4), fine- to coarse-grained, poorly sorted sands with petrological features that are comparable to the alluvial and drowned channel sands described above, oc-

© 2001 INIST-CNRS. Tous droits de propriété intellectuelle réservés. Reproduction, représentation et diffusion interdites. Loi du 01/07/92. Articles 5, 6 et 7 des CGV.

cur in the lower portion of cores E-1 and S-71 located to the east of core S-73 (Figure 1). However, these sands contain a higher proportion of fine sands, and are interbedded with occasional thin (centimeter to decimeter) stiff muds. These sands and stiff muds are ~20–30 m thick in cores E-1 and S-71. A radiocarbon date in muds at the top of this facies in core S-71 indicates that this facies was deposited before 11,000 years BP. These sand and stiff mud sequences are interpreted to have been deposited along the flanks of a river channel near the coast. The presence of occasional marine fossils and shell fragments suggests that the river valley was periodically inundated by the sea.

Flood Plain Muds

Grayish green (10GY 5/2) to grayish olive (10Y 4/2) sandy stiff muds occur in the upper portion of the late Pleistocene sequence in three cores (S-67, S-69, S-73). Sands occur as dispersed, matrix-supported grains, or as discrete beds (to 20 cm thick) and lenses. Irregularly shaped calcareous nodules (1 mm to 3 cm) are ubiquitous. Reddish brown iron-rich beds, lenses and aggregates are common. Black, vegetal-rich laminae are also present, and are usually fissile and contorted. Mottling and root traces occur throughout. Sandstone pebbles occur locally. In some sections, interbedded sandstones are current-ripple laminated. This facies ranges in thickness from 0.3 to 4.4 m. Radiocarbon dates from this facies indicate an age ~35,000 to 11,000 years BP. Fauna and flora are sparse to absent. These sandy muds are interpreted to be channel overbank and crevasse-splay deposits which accumulated in shallow ephemeral lakes and/or playas in close proximity to distributary channels (*cf.* Butzer, 1976; Abdel Wahab and Stanley, 1991), under generally arid conditions (*cf.* Reineck and Singh, 1980; Collinson, 1986; Gustavson, 1991).

Previous investigations in the north-central Nile delta (Arbouille and Stanley, 1991; Stanley *et al.*, 1992) recognized two distinctive stiff muds facies (overbank and interdistributary lagoon facies). In the study area there are fewer mud strata in the cores, and no more than one layer of stiff mud per boring. Only the stiff mud facies of overbank origin is recognized in this region.

Late Pleistocene to Early Holocene Transgressive Sands

Olive gray (5Y 3/2) to yellowish brown (10YR 4/2), fine- to coarse-grained, rather poorly sorted sands occur above the late Pleistocene sands and stiff muds in most cores of the northern study area (Figure 4). These sands are primarily composed of unstained quartz (Table 1); common accessory components include heavy minerals, shell fragments and verdine/glauconite. In the western part of the study area (S-72, S-74, S-75, S-76, Figure 1), undifferentiated carbonate and shell fragments comprise as much as 35% of the sand fraction. This facies ranges from 0.5 to 17 m thick, and radiocarbon dates suggest that the sands were deposited from ~15,000 to 8,000 years BP. Fauna, although generally sparse, includes gastropods, pelecypods, ostracods and foraminifera. Several previous Nile delta studies to the east (*e.g.* Coutellier and Stanley, 1987; Arbouille and Stanley, 1991; Stanley *et al.*, 1992) have interpreted this facies to be marine transgressive sands which were deposited during the last rapid rise in sea level (Flandrian transgression). These sands are the product of reworking of earlier marine deltaic and shallow shelf deposits which resulted in concentration of sands. The westward increase in carbonate content in this facies has been documented by Stanley and Hamza (1992): the increase in marine carbonates relative to terrestrial siliciclastics is the result of the decreased influence of the River Nile system immediately to the west of the study area.

Holocene Sediment Types

Nile delta sediments of Holocene age began to accumulate ~8,000–7,000 years BP as the rate of sea-level rise began to decrease (Mörner, 1976; Lighty *et al.*, 1982; Fairbanks, 1989; see sea-level curve in Figure 4). The distribution of Holocene lithofacies in the study area are laterally variable: open marine bay facies are more prominent in the western sector; thick marsh deposits occur in the eastern sector; and delta-front and nearshore/coastal facies only occur in the Rosetta promontory sector (Figure 4). Unlike the northeastern Nile delta (Coutellier and Stanley, 1987), there is no complete progradational (coarsening-upward, prodelta to delta plain) sequence in the study area. Depositional sequences examined here tend to be aggradational and retrogradational, as in the north-central delta (Wilgus *et al.*, 1988; Arbouille and Stanley, 1991; Stanley *et al.*, 1992). Generally lower proportions of smectite in the Holocene section than in the underlying Pleistocene units indicate that Holocene sediments were, for the most part, deposited in marine-in-

© 2001 INIST CNRS. Tous droits de propriété intellectuelle réservés. Reproduction, représentation et diffusion interdites. Loi du 01/07/92. Articles 5, 6 et 7 des CGV.

fluenced environments (ABU-ZEID and STANLEY, 1990; ABDEL WAHAB and STANLEY, 1991).

An unconformity separates the Holocene from underlying alluvial or marine transgressive sands (SESTINI, 1989; BERNASCONI *et al.*, 1991; STANLEY *et al.*, 1992). In the present study area, lag deposits comprising shells, coarse sands, and rounded, flattened fine sandstone pebbles occur at or just above this hiatus in many cores. Radiocarbon dates indicate that this lacuna is larger in the southern and western part of the study area.

Delta-Front Muds, Silts and Sands

Light olive gray (5Y 5/2) to yellowish gray (5Y 7/2) to dark gray (N3) interbedded muds, silts and sands occur in two cores (S-59 and S-64) in the vicinity of the Rosetta promontory. Translucent to transparent quartz is the principle silt- and sand-size constituent; common accessory components include heavy minerals, shell fragments, mica, plant debris and small pebbles (Table 1). PIMMEL and STANLEY (1989) demonstrated that verdine/glauconite, comprising up to 44% of sand in this facies in the northeastern delta, serves as a key indicator of shallow marine deposits. Sediments range from distinctively laminated to highly bioturbated; where undisturbed, they are planar-bedded and planar to trough cross-laminated. This facies is about 6.5 m thick. Radiocarbon dates indicate that delta-front sediments were deposited between ~4,000 and 2,200 years BP. Fauna includes benthic foraminifera, ostracods, sponge spicules and molluscs. Cross-laminated sands and silts, as well as the highly diverse fauna and glauconite, suggest that these sediments accumulated in shallow open marine conditions (COUTELLIER and STANLEY, 1987; BERNASCONI *et al.*, 1991; STANLEY *et al.*, 1992).

Marine Bay Muds

Olive gray (5Y 3/2), grayish black (N2), to greenish black (5 GY 2/1) soft, massive and homogenous muds occur near the base of the Holocene sequence in five cores (S-72 to S-76, Figures 1 and 4), just to the southeast of Abu Qir ridge. Common components include light and heavy minerals, micas, and shells (Table 1). Horizontal and uneven laminae are commonly observed in muds; stratification, in some cases, is the result of concentrations of fossils (Figure 5A). Marine bay mud sections range in thickness from 1.2 to 7.0 m. Radiocarbon dates indicate that this facies was deposited primarily between ~7,000 and 5,000 years BP. The muds are generally fossiliferous, with bivalves, gastropods and foraminifera as the most common taxa. As in lagoons, molluscs are commonly abundant and may occur as dense shell layers; however, shells in marine bay facies (Figure 5A) tend to be smaller than those in lagoons (Figure 5B). Molluscan assemblages from the bay facies indicate open marine conditions, with water depths ranging from ~5 to 7 m (M.P. BERNASCONI, *written communication*, 1991).

Carbonate pebbles commonly occur in the marine bay muds and are composed of soft to semi-lithified, irregularly-shaped calcareous siltstones and grainstones. Thin-section analysis shows that these pebbles were derived from the adjacent Abu Qir carbonate ridge (EL FAYOUMY *et al.*, 1975; STANLEY and HAMZA, 1992). The pebbles were probably washed from the ridge into the bay during storms.

Lagoon Muds

Olive gray (5Y 3/2) to dark gray (N3), vegetal-rich lagoon muds and silts occur in most cores of the study area. They are primarily composed of light and heavy minerals, mica, plant debris and verdine/glauconite (Table 1); some intervals consist almost entirely of molluscs (Figure 5B). Bedding may be intact or completely obscured by bioturbation. Where undisturbed, a variety of bedding features include: horizontal and wavy lamination, small-scale ripple cross lamination, and lenticular to flaser bedding (STANLEY *et al.*, 1992, their Figure 3). The thickness of lagoon deposits ranges from 2 to 6 m. Radiocarbon data indicate that lagoon deposits accumulated from ~5,000 years BP to the present. Fauna and flora include characteristic ostracods (PUGLIESE and STANLEY, 1991), benthic foraminifera (EL-WAKEEL *et al.*, 1970; KULYK, 1987), molluscs (BERNASCONI *et al.*, 1991), sponge spicules and diatoms. Molluscan paleocommunity analysis indicates accumulation in brackish water conditions (M.P. BERNASCONI, *written communication*, 1991).

Two lagoon subfacies are distinguished primarily on the basis of the petrology of interbedded sands (ARBOUILLE and STANLEY, 1991): fluvially-influenced and storm wash-over. These two sandy lagoon subfacies are described in subsequent sections describing sand facies.

Marsh Peats and Vegetal-rich Muds

Thick sequences of dark gray (N3), plant-rich, intensely bioturbated, silty muds and peats occur

© 2001 INIST CNRS. Tous droits de propriété intellectuelle réservés. Reproduction, représentation et diffusion interdites. Loi du 01/07/92. Articles 5, 6 et 7 des CGV.

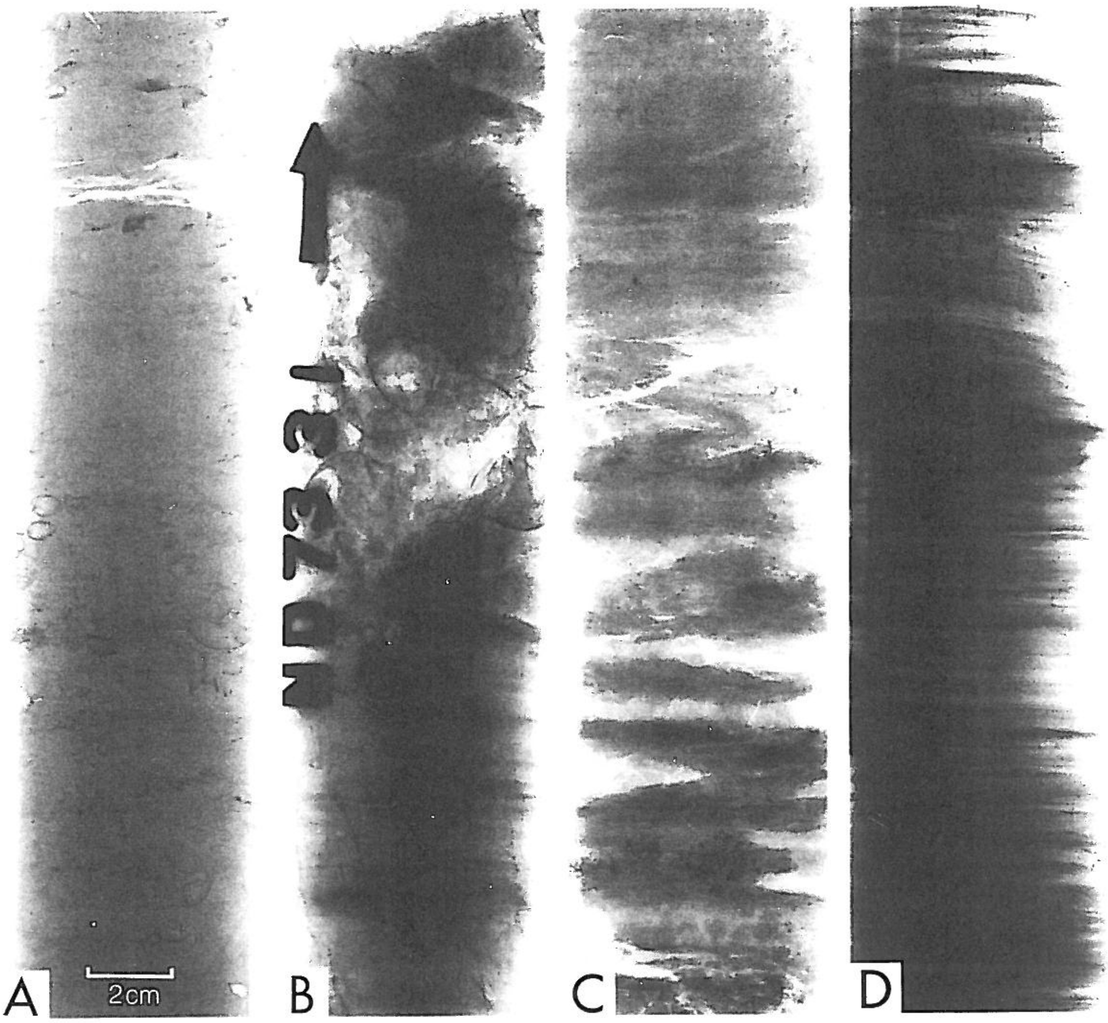

Figure 5. X-radiograph prints of representative facies from Smithsonian borings. (A) Open marine bay, showing soft, homogeneous fossiliferous mud; fossil shells tend to be smaller (~0.3–1 cm) and more evenly dispersed in bay than in lagoon facies (boring S-75, ~13.6 m core depth). (B) Lagoon, showing cross-lamination in the lower silty mud portion and a shell layer in the central portion; fossil shells (mostly *Cardium*) tend to be larger (1–2 cm) than in marine bay facies and commonly occur in concentrated layers (S-73, ~4.7 m depth). (C) Marsh, showing interlaminated vegetal-rich layers (dark) and peaty muds (light); this lamination is only apparent in X-rays (S-66, ~11.9 m depth). (D) Silt plain, showing typical thin, parallel to cross-laminated silts and muddy silts (S-72, ~3.2 m depth). Bar scale = 2 cm.

in eight cores (S-51, S-58, S-60, S-61, S-62, S-63, S-66 and S-68, Figure 1) in the southeastern study area (Figure 4). Peats (semicarbonized plant remains which accumulated *in situ* under chemically reducing conditions) are composed of >65% vegetal matter, whereas marsh muds are composed of 15–65% vegetal matter (Howa and Stanley, 1991). Root traces are ubiquitous, and pyrite is common to abundant (up to 35% in cores S-58 and S-66) in this facies. Fauna includes sponge spicules and diatoms; molluscs are less abundant than in the lagoon facies. Vegetal-rich layers, ranging in thickness from 2 cm to 5 m, are interbedded with organic-rich muds (Figure 5C). Marsh facies range in thickness from 1.5 to 14 m; peats in the study area include the thickest yet recovered from the Nile delta (*cf.* Howa and Stanley, 1991). Radiocarbon dates indicate that

© 2001 INIST CNRS. Tous droits de propriété intellectuelle réservés. Reproduction, représentation et diffusion interdites. Loi du 01/07/92. Articles 5, 6 et 7 des CGV.

marsh deposition took place between ~7,500 and 3,000 years BP. HOWA and STANLEY (1991) have pointed out that: (1) ancient marshes were deposited in settings similar to extent marshes (*i.e.* along the landward margin of coastal lagoons); (2) marsh distribution is linked to the location of major distributary channels; and (3) marshes developed in areas of low clastic input.

Silt-Plain Silts

Grayish brown (5YR 3/2) muddy silts occur in seven cores (S-51, S-56, S-58, S-60, S-66, S-70, S-72). Laminae and small lenses (0.5–2.0 cm thick) of fine sands and silts are interbedded with the muddy silts throughout the section (Figure 5D). Wavy lamination and small-scale ripple cross bedding are common (Figure 5D). The sand fraction is primarily composed of quartz; mica is a significant accessory component. The proportion of heavy minerals is usually very low. The thickness of the silt-plain facies ranges from 2 to 9 m. Radiocarbon dates indicate that this facies ranges in age from ~2,700 years BP to near-present. This facies, essentially devoid of fossils and fossil fragments, is interpreted to have been deposited as overbank deposits which accumulated during River Nile floods prior to closure of the Aswan Dam.

Holocene Sand Facies

Six sand facies of Holocene age are recognized in the study area (Figure 4): river-mouth, nearshore marine/beach, backshore sand-flat/dune, lagoon, fluvial, and kôm.

River Mouth Sands. Light olive gray (5Y 5/2) to olive gray (5Y 3/2) fine- to medium-grained sands comprise a 46 m thick, all-sand section in core S-65, near the head of Rosetta promontory (Figure 1). STANLEY and CHEN (1991), using combined composition and stained-grain analyses on this 46 m interval, differentiated 10 m of river mouth sands in the lower portion and 36 m of beach sands in the upper portion. Like most river sands, those in the lower 10 m contain a high proportion of partially stained grains and light minerals, but unlike most river sands, there is a relatively high content of heavy minerals and a minor proportion of marine biogenic components (Table 1). Because of the lack of sufficient calcium carbonate, no radiocarbon dates could be obtained. We interpret the sands in the lower part of S-65 to have been deposited near the mouth of a river which was periodically influenced by marine conditions.

Nearshore Marine to Beach Sands. Yellowish gray (5Y 7/2 to 5Y 8/1) mostly fine- to medium-grained sands occur in four cores (S-59, S-63, S-64, S-65). These sands are characterized by relatively low proportions of partially stained quartz, and high proportions of heavy minerals. Verdine/glauconite is a common accessory component. This facies ranges from ~5 to 36 m in thickness. Radiocarbon dates indicate that these sands were deposited from ~6,500 years BP to the present. Shells are sparse and occur mostly as fragments. The low proportions of stained quartz and high proportions of heavy minerals are characteristic of sands deposited in a swash zone where they have been extensively reworked (STANLEY *et al.*, 1992). Glauconite indicates that these sands accumulated, at least in part, in a shallow marine environment (PIMMEL and STANLEY, 1989).

Backshore, Sand-flat and Dune Sands. Grayish orange (10YR 7/4) to yellowish brown (10YR 4/2), very fine- to fine-grained, well-sorted sand occurs in the upper portion of two cores (S-59 and S-64), west of Rosetta promontory. Quartz is the dominant mineral constituent; heavy minerals are an important accessory component (Table 1). Other accessory components include mica, gypsum, and lithic and some shell fragments. It is of note that proportions of heavy minerals, shell fragments and verdine/glauconite are lower than in coastal sands. Radiocarbon dates indicate that this facies accumulated from ~2000 years BP to present. The relatively high proportion of heavy minerals is interpreted to be the result of selective removal of light minerals by wind, and consequent concentration of denser minerals.

Lagoon Sands. Pale yellowish brown (10YR 6/2) to yellowish gray (5Y 7/2) very fine- to fine-grained, moderately to well-sorted sands occur as beds and lenses within mud-rich lagoon facies in most cores. Quartz is the primary constituent; mica is a significant accessory component. Other accessory components include shell fragments, aggregates, verdine/glauconite, pyrite and gypsum. Sand layers in lagoon facies range from a few millimeters to 5 cm thick.

Two subfacies of lagoon sands are recognized: fluvial-influenced and storm wash-over (Table 1; see also STANLEY and CHEN, 1991). Of the two, storm wash-over sands (*cf.* HAYES, 1979) which were deposited in a lagoon environment contain relatively higher percentages of fossils and verdine/glauconite. In contrast, fluvial-influenced sands, which were deposited in a more terrestrial

© 2001 INIST CNRS. Tous droits de propriété intellectuelle réservés. Reproduction, représentation et diffusion interdites. Loi du 01/07/92. Articles 5, 6 et 7 des CGV.

environment, comprise a higher percentage of mica and plant debris, and a lower percentage of verdine/glauconite and fossils. Nevertheless, the small proportions of brackish water tests (ostracods, foraminifera) indicate that these fluvial-dominated sands were deposited, at least in part, in lagoon settings that were connected to the sea.

Fluvial Channel Sands. Olive gray (5Y 3/2) to grayish olive (10Y 4/2) fine-grained, moderately to poorly sorted sands occur in the upper portion of seven cores (S-58, S-60, S-66, S-67, S-69, S-71, S-73). The proportion of partially stained quartz is relatively high (Table 1), but in contrast to late Pleistocene alluvial sands, this facies is characterized by the absence of coarse, iron-stained, rounded quartz. Quartz is the main constituent; accessory components include heavy minerals, mica, gypsum, and aggregate. The thickness of this facies ranges from 1.5 to 6.5 m. Radiocarbon dates have established that these fluvial deposits accumulated between ~6,500 to 2,500 years BP to the west of Idku lagoon (S-71, S-73), and ~2,500 years BP to present to the east-southeast of Idku lagoon (S-58, S-60, S-66, S-67, S-69). These sands are interpreted to be river channel and crevasse-splay deposits.

Kôm Sands. Moderate yellowish brown (10YR 5/4), fine- to medium-grained, moderately sorted sands form a series of hills (northwest-southeast oriented) to the south and southeast of Idku lagoon (Figure 2). While no sediment borings were drilled in the kôms, two near-surface kôm samples were collected and petrologically analyzed (Figure 2). Kôm sands are primarily composed of highly-stained quartz (Table 1). Accessory components include aggregates and gypsum; the proportion of heavy minerals is usually very low. The thickness and age of these kôms are yet to be determined. The origin of these sands is controversial: they have been described as "older coastal dunes" (El Fattah and Frihy, 1988; Sestini, 1989), and as "residual sands (Canopic upper beds)" (El-Fayoumy *et al.*, 1975). The presence of highly stained quartz and sand-sized aggregates suggest that the sands are fluvially derived. Gypsum and other attributes such as overall shape and height of kôms suggest that these features formed as dunes by wind transport of fluvial silt and sand.

FACIES AS RELATED TO SEA LEVEL, SUBSIDENCE, AND CLIMATE

The above analyses highlight the diversity of late Quaternary marine and nonmarine sediment types in the northwestern Nile delta. A synthesis of the laterally variable lithofacies sequences is represented by three generalized sequences from three sectors of the study area (Figure 4). In the following sections, an attempt is made to place these late Quaternary lithofacies sequences in a comprehensive stratigraphic and paleogeographic context. To do so requires that each facies be examined with respect to principal factors which control lithofacies distribution. Here, lithofacies distributions in time and space are considered in terms of sea level, subsidence and climate. A fourth major factor, sediment transport processes, is considered in later sections.

Sea-level Factor

The late Quaternary lithofacies in the Nile Delta study area were deposited during the most recent eustatic sea-level cycle: from the last Pleistocene high-stand (~35,000 to 30,000 years BP), to the last Pleistocene low-stand (~20,000 to 18,000 years BP), to the present high-stand (*cf.* eustatic curves of Curray, 1965; Mörner, 1976; Lighty *et al.*, 1982; Fairbanks, 1989). Tide-gauge and historic records indicate continued rise in sea level in the Alexandria coastal region during this century (El-Fishawi and Fanos, 1989).

The relationship between lithofacies and sea level is as follows:

(1) Alluvial to shallow marine sands and some stiff muds accumulated from earlier than ~30,000 years to 18,000 years BP, during the last Pleistocene sea-level high stand and last major eustatic lowering.

(2) Alluvial sands with local drowned valley sands and stiff muds accumulated from ~18,000 to 11,000 years BP, during the last major low-stand and the early phases of the subsequent, very rapid sea-level rise (Figure 4). The former Nile delta shoreline migrated as much as 50 km to the north of the present coast during this time, *i.e.* just landward of the present-day shelfbreak (Summerhayes *et al.*, 1978; Maldonado and Stanley, 1979; Abdel Wahab and Stanley, 1991).

(3) Fluvial overbank muds accumulated from ~15,000 to 11,000 years BP, during the rapid rise in sea-level, which included the time of the Bölling-Alleröd phase (*cf.* Fairbanks, 1989).

(4) Marine transgressive sands accumulated from ~15,000 to 8,000 years BP, as sea level continued to rapidly rise. This rapid rise caused the coastline to retrograde southward of the present-

© 2001 INIST CNRS. Tous droits de propriété intellectuelle réservés. Reproduction, représentation et diffusion interdites. Loi du 01/07/92. Articles 5, 6 et 7 des CGV.

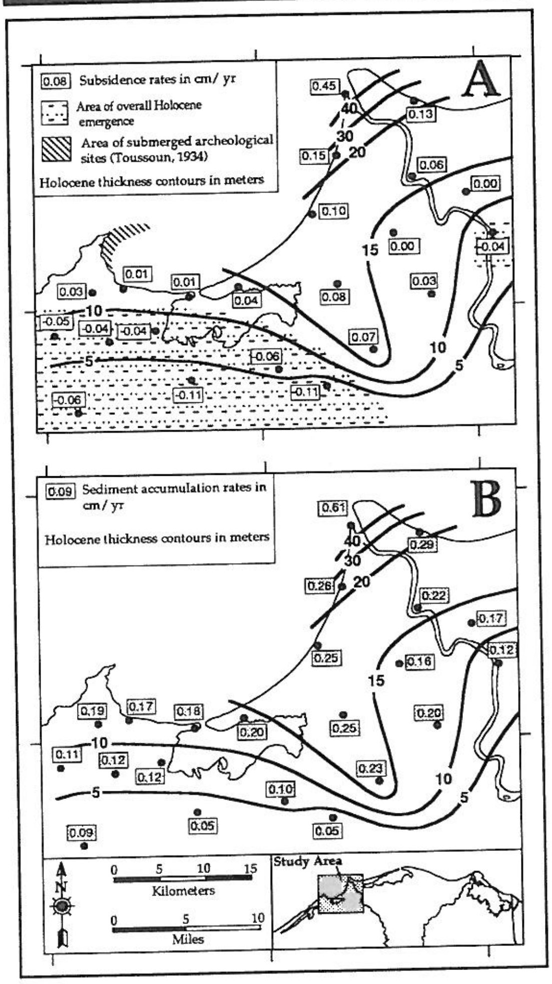

Figure 6. Isopachous maps of the total Holocene thickness (contours in meters). (A) Map showing long-term averaged Holocene subsidence rates in cm/yr. Sector denoted by negative subsidence rate values is one of overall Holocene emergence. (B) Map showing long-term averaged Holocene sediment accumulation rates in cm/yr.

day Nile delta shoreline. An unconformity occurs at the base of the transgressive sands as a result of wave erosion and reworking of late Pleistocene sediment as the shoreline onlapped landward (southward).

(5) An unconformity also occurs at the top of the transgressive sands. Radiocarbon dates indicate that this lacuna is variable in duration. In particular, this hiatus continued to be a surface of nondeposition and (or) erosion into the early Holocene, especially in the southern and western portion of the study area.

(6) Marine bay muds and fluvial sands accumulated in the western sector of the study area; marsh muds and peats accumulated in the eastern sector of the study area; and beach sands accumulated in the Rosetta promontory sector from ~7,000 to 5,000 years BP (Figure 4). By ~7,500 years BP the rate of sea-level rise decelerated such that the rate of sediment input began to predominate over the rate of sea-level rise; consequently, aggradation and progradation of Holocene Nile delta sediments onto the unconformity commenced.

(7) From ~5,000 years BP to the present, lagoon muds, marsh muds and peats, and fluvial sands accumulated in the western and eastern portions of the study area, whereas delta-front muds, silts and sands, and nearshore marine/coast sands accumulated in the Rosetta promontory. During this period, sea level rose from about −5 m to the present position (LIGHTY *et al.*, 1982).

Subsidence Factor

Lithofacies distributions can be affected by lowering of land surface (subsidence) relative to sea level in a similar way as it can by a rise in sea level relative to land surface. It is, therefore, of concern to distinguish the effects of these two factors (eustacy *vs.* subsidence) which control sediment distribution in time and space. An isopachous map of the total Holocene section (Figure 6) is useful in differentiating these two controlling factors.

Figure 6 shows that thickness contours generally are subparallel to the present-day coast and that Holocene sediments gradually thicken seaward. These trends would be expected along a coastline where sediment distribution is controlled by steadily rising sea level and (or) isostatic subsidence. Isopachous contours, however, deviate locally from the present shoreline trend. For example, contours in the Rosetta promontory (from data in borings S-59, S-64, S-65) indicate that Holocene sediment rapidly thicken seaward (from 20 to 35 m within a distance of 7 km); this marked thickening may be attributed to either isostatic subsidence and (or) fault-controlled displacement. In this respect, it is recalled that there is a thick, extensive Plio-Pleistocene age sediment wedge, the Rosetta Cone, seaward of the promontory (ROSS and UCHUPI, 1977). A marked V-shaped contour pattern determined by borings S-61 and S-62 south-southwest of the Rosetta

© 2001 INIST CNRS. Tous droits de propriété intellectuelle réservés. Reproduction, représentation et diffusion interdites. Loi du 01/07/92. Articles 5, 6 et 7 des CGV.

promontory may record both subsidence and pre-Holocene valley erosion.

Long-term subsidence rate has been calculated for each of the twenty-two cores in the study area (*cf.* method of STANLEY, 1990). To obtain conservative values, calculations assume that (1) Holocene sediments began to accumulate at 7,500 years BP (*cf.* STANLEY, 1988, 1990); (2) sea level was −12 m at 7500 years BP (*cf.* LIGHTY *et al.*, 1982); (3) sediment compaction has not significantly modified lithofacies thickness trends (based on the field measurement of sediment strength in cores). Subsidence rate calculations involve determination of total Holocene sedimentary thicknesses for each boring, substraction of 12 m of sediment thickness to compensate for lower sea-level stand at 7,500 years BP, and division of remaining sediment thickness by 7,500 years. For example, core S-62 has total thickness of 17.5 m. Thus, 17.5 m − 12 m = 5.5 m, or 550 cm of accumulation in 7,500 years. From these values, a lowering rate of 0.07 cm/yr (70 cm/1,000 yr) is calculated.

Calculated long-term subsidence rates increase seaward from −0.06 cm/yr in the southwest study area to 0.45 cm/yr in the north (Figure 6A). It is probable that negative values in the southwestern sector record overall emergence during the Holocene. Emergence (also determined for the Alexandria region by EMERY *et al.*, 1988) would suggest the presence of a hiatus or hiatuses somewhere in the section (Figure 6A). Radiocarbon dates from study area cores demonstrate that the only significant hiatus occurs at the base of the Holocene, particularly in this southwestern sector. In contrast, the Rosetta promontory has been affected by subsidence rates as high as 0.45 cm/yr; when compared to the other northern Nile delta studies, subsidence rates of this magnitude have only been reported in the Manzala lagoon region (COUTELLIER and STANLEY, 1987). Calculated rates for the northwestern portion of the study area are low, but indicate overall subsidence.

It is of note that the presence of ruins of the ancient Hellenistic city of Canopus in Abu Qir Bay (Figure 6A; TOUSSOUN, 1934) now lie as much as 5 m below sea level. TOUSSOUN (1934) assumed that these Hellenistic (~500 BC and younger) ruins were originally as much as 3 m above sea level, which would mean that they were lowered 8 m with respect to sea level during the past 2,500 years. According to most eustatic curves (*cf.* LIGHTY *et al.*, 1982; FAIRBANKS, 1989), sea level

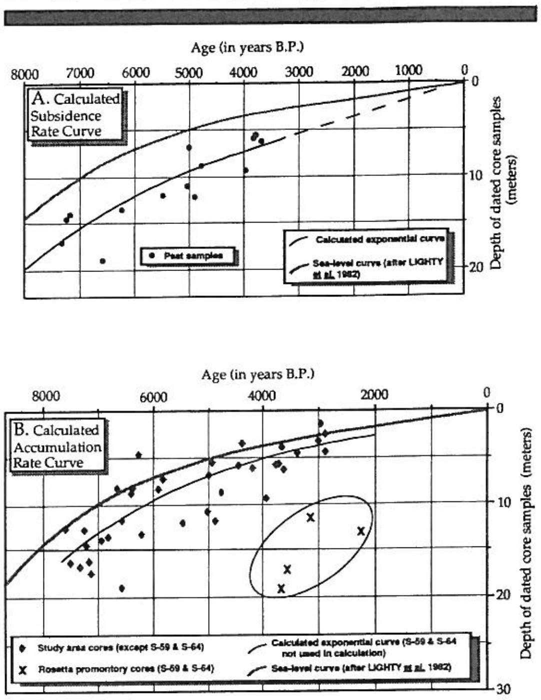

Figure 7. Graphs showing core depth versus radiometric age of: (A) 15 peat layers from 8 cores; and (B) 40 sediment samples from 21 cores. Exponential curves were calculated for these two data sets. Superimposed on the calculated curves is a generalized eustatic sea-level curve (from Lighty *et al.*, 1982), where depth is in meters below sea level. Note that calculated curves for both A and B lie below the eustatic curve. Note also that the Rosetta promontory samples (shown as X's) lie well below the remainder of the samples of similar age. Error in dates (as reported by Beta Analytic Inc.) range from ±60 to ±140 years.

has risen ~2.5 m during the past 2,500 years. This suggests that the ruins of Canopus may have subsided at a rate of 0.22 cm/year, which is significantly higher than rates to the south (Figure 6A), and approaches those rates recorded in the Rosetta promontory to the east.

The radiocarbon dates from fifteen peat layers in eight cores have been plotted versus their depth below present mean sea level (Figure 7A). All cores containing peats are from the eastern sector of the study area. It is assumed that these peats accumulated at, or very close to, sea level. A calculated exponential curve from these peat samples can be compared to a general eustatic sea-level curve (LIGHTY *et al.*, 1982), the latter showing an average rise in sea level of ~0.10 cm/yr during the past 5,000 years. Our calculated curve based on the fifteen radiocarbon-dated peats lies below the sea-level curve. The exponential

© 2001 INIST CNRS. Tous droits de propriété intellectuelle réservés. Reproduction, représentation et diffusion interdites. Loi du 01/07/92. Articles 5, 6 et 7 des CGV.

curve has been extrapolated to the present mean sea level stand, and is essentially linear with a slope of ~0.18 cm/yr. The spacing between the two curves increases with time and depth in core. This suggests that, in general, the study area has undergone some subsidence, *i.e.* lowering relative to sea level on the order of 0.08 cm/yr (0.18 cm/yr −0.10 cm/yr = 0.08 cm/yr). This lowering, which can be accounted for by isostatic lowering and minor compaction, is similar to earlier calculated subsidence values for this sector (*cf.* STANLEY, 1990).

From the above considerations, it is apparent that the petrologically variable Holocene sequences in the study area accumulated in a sector of the delta which (with the notable exception of the Rosetta promontory) has undergone only modest amounts of subsidence. Holocene subsidence rates in the study area were such that open marine facies (delta-front and marine bay) are quite limited in vertical and lateral extent (Figure 4). In consequence, complete coarsening-upward deltaic sequences of Holocene age (prodelta to delta plain), as are found in the more rapidly subsiding northeastern delta (COUTELLIER and STANLEY, 1987), did not form in the northwestern delta. The Rosetta promontory region is a marked exception to the remainder of the study area; subsidence rates to 450 cm/1,000 years are some of the highest so far recorded in the northern Nile delta. Whether this area of rapid subsidence is fault-controlled or marks the location of a hinge line, the weight of the large Rosetta Cone undoubtedly is an essential factor to the exceptionally high subsidence.

Climatic Factor

Climatic oscillations can directly or indirectly affect sea-level fluctuations, coastline evolution, river channel migrations, and sediment distribution. Thus, in order to fully understand late Quaternary Nile delta paleogeography, it is important to differentiate the role of climate from the other factors that control sediment distribution. The late Quaternary climatic history of the eastern Sahara and Nile valley region during the past 35,000 years can be summarized as follows: from ~35,000 to 25,000 years BP climate was arid; from ~25,000 to 20,000 years BP conditions were somewhat more humid; from ~20,000 to 12,500 years BP climate was generally cool and dry; from ~12,500 to 5,000 years BP climate was more humid resulting in high floods; and from ~5,000–4,000 years to the present, climate has been arid (ADAMSON *et al.*, 1980; PAULISSEN and VERMEERSCH, 1989; PETIT-MAIRE, 1989).

Several lithofacies can be related to syndepositional climatic conditions. Medium to coarse, poorly sorted, iron-stained, well rounded sands of late Pleistocene age (particularly those which accumulated between ~20,000 and 12,500 years BP) were deposited under arid conditions by a seasonally dry, braided river system (ADAMSON *et al.*, 1980). During periods of aridity, vegetation cover (which tends to stabilize sediments) in the Nile headwater region was sparse so that large volumes of coarse sediment were available for transport to the delta, especially during flood season. Overbank muds of Pleistocene age (~35,000–23,000 and ~15,000–11,000 years BP), were deposited locally in ephemeral interchannel depressions. Formation of calcareous nodules and gypsum in these flood-plain muds suggests repeated seasonal wetting and drying in an arid to semiarid climate (GUSTAVSON, 1991).

The Holocene lithofacies in the study area (~7,500 years BP to the present) provide evidence of climatic oscillations: (1) reduced proportions of iron-stained, coarse sands in Holocene river channel deposits indicate more humid conditions; (2) the distribution of discrete fluvial lithosomes (Figure 4) of Holocene age record a change from a seasonally dry, braided river to a perennial, meandering river system; and (3) formation of very thick peats, which accumulated from ~7,500 to 5,000 years BP may suggest warm, humid conditions. These observations concur with those made in the delta regions to the east (ARBOUILLE and STANLEY, 1991; STANLEY *et al.*, 1992).

In our view, climate has influenced sediment composition and facies distribution in the Nile delta study area, but to a lesser extent than either eustatic sea level or subsidence. For instance, the overall change from late Pleistocene alluvial to Holocene marine and coastal deposits records the change from a major sea level low-stand to a high-stand. Moreover, variable Holocene sediment thicknesses and lithofacies sequences (Figure 6) in the study area are attributed to different subsidence histories.

RATE OF SEDIMENT ACCUMULATION

Holocene sediment accumulation rates (Figure 6B) are calculated to more accurately interpret facies distribution in time and space and, more

© 2001 INIST CNRS. Tous droits de propriété intellectuelle réservés. Reproduction, représentation et diffusion interdites. Loi du 01/07/92. Articles 5, 6 et 7 des CGV.

specifically, to distinguish the relative effects of differential subsidence and sea level on the sediment accumulation rates. Accumulation rates have been calculated in two ways, as described below.

Long-term averaged rates of sediment accumulation were calculated for each of the twenty-two Smithsonian cores in the study area. Calculations first involved determination of core depth of each of the 52 radiocarbon-dated samples, and then division of this core sample depth by its radiocarbon age. For example, core S-61 has a radiometric age of 7,310 yr at 17.1 m. Its calculated average accumulation rate is 1,710 cm per 7,310 years, or 0.23 cm/yr (230 cm/1,000 yr). This calculation was done for 7 borings. In most cores (15 of the 22), radiocarbon dates near the base of the Holocene section are absent, or are anomalously young (recording an extended late Pleistocene to early Holocene hiatus), or are considered unreliable. Calculations for these 15 borings were made on the basis of lateral correlation with the 7 dated cores, where the base of the Holocene cores were dated from ~7,500 to 7,200 years BP (*cf.* Stanley, 1990). Thus for these fifteen cores, the total Holocene core thickness was divided by 7,500 years to calculate their interpolated accumulation rate.

Holocene sediment accumulation rates across the study area (Figure 6B) generally increase from south (0.05 cm/yr or 50 cm/1,000 yr) to north (0.61 cm/yr or 610 cm/1,000 yr). That sediment accumulation rates are anomalously high in the Rosetta promontory (0.25–0.61 cm/yr; Figure 6B) is revealed in Figure 7B. Comparison of Figures 6A and 6B shows that there is a close correlation between long-term average sediment accumulation rates and subsidence rates. This implies that sedimentation has kept pace with or has exceeded subsidence, even in the Rosetta promontory where subsidence rates are the highest.

Changes in sediment accumulation rates over time are determined, using 40 radiocarbon-dated samples from 21 cores. A graph showing depths of dated samples versus age of these samples (Figure 7B) reveals a marked decrease in sediment accumulation rates from ~7,500 to 5,000 years BP, and then a more gradual decrease in rates from ~5,000 to 3,000 years BP. These trends are highlighted by a calculated exponential curve. The dispersal of data points may be due to the irregular surface of the pre-Holocene on which Holocene sediments were deposited. Samples from the Rosetta promontory (shown as x's in Figure 7B) were not used in calculating the curve.

The calculated accumulation curve is subparallel with, but lies below, the general eustatic sea-level curve (*cf.* Lighty *et al.*, 1982). The subparallel trend of the accumulation curve with the sea-level curve indicates that major changes in sediment accumulation rates are generally coincident with changes in rates of sea-level rise. This would support our contention that Holocene sedimentary conditions in the study area are primarily controlled by rate of eustatic sea-level fluctuations. However, the four samples from the Rosetta promontory cores do not follow the general trend of the other 36 dated samples (Figure 7B). The position of these four points, well below the sea-level curve, demonstrates that subsidence has been a major factor in determining sedimentary conditions in the Rosetta promontory.

An average regional sediment accumulation rate of 0.14 cm/yr for the past 5,000 years has been estimated from the overall slope of the calculated curve in Figure 7B. A value of 0.04 cm/yr is obtained if we subtract the effects of sea-level rise (0.10 cm/yr) from the averaged accumulation rate (0.14–0.10 cm/yr). This value of 0.04 cm/yr can best be explained by subsidence. It is of note that the 0.04 cm/yr value is identical with the calculated average subsidence rate for the Burullus lagoon region (Arbouille and Stanley, 1991; Stanley *et al.*, 1992).

REGIONAL LITHOFACIES CORRELATION AND GEOMETRY

Petrologic, faunal, and radiometric information from all study area cores is applied to establish core-to-core correlations and to distinguish late Quaternary lithofacies distributions in time and space. Correlations among borings and regional lithofacies distribution trends take into account the controlling factors discussed in the previous section as well as sediment transport processes. Salient features of lithofacies distributions are depicted in Figures 8 and 9, and are described below, from oldest to youngest:

(1) Thick sections of late Pleistocene sands (>35,000–11,000 years BP) occur throughout the study area. Most of these medium to coarse sands are interpreted to be braided river deposits, with some intercalated nearshore marine and beach sands (especially in the lower portions).

(2) A thick section of late Pleistocene drowned channel sands (~18,000–11,000 years BP) occurs

© 2001 INIST CNRS. Tous droits de propriété intellectuelle réservés. Reproduction, représentation et diffusion interdites. Loi du 01/07/92. Articles 5, 6 et 7 des CGV.

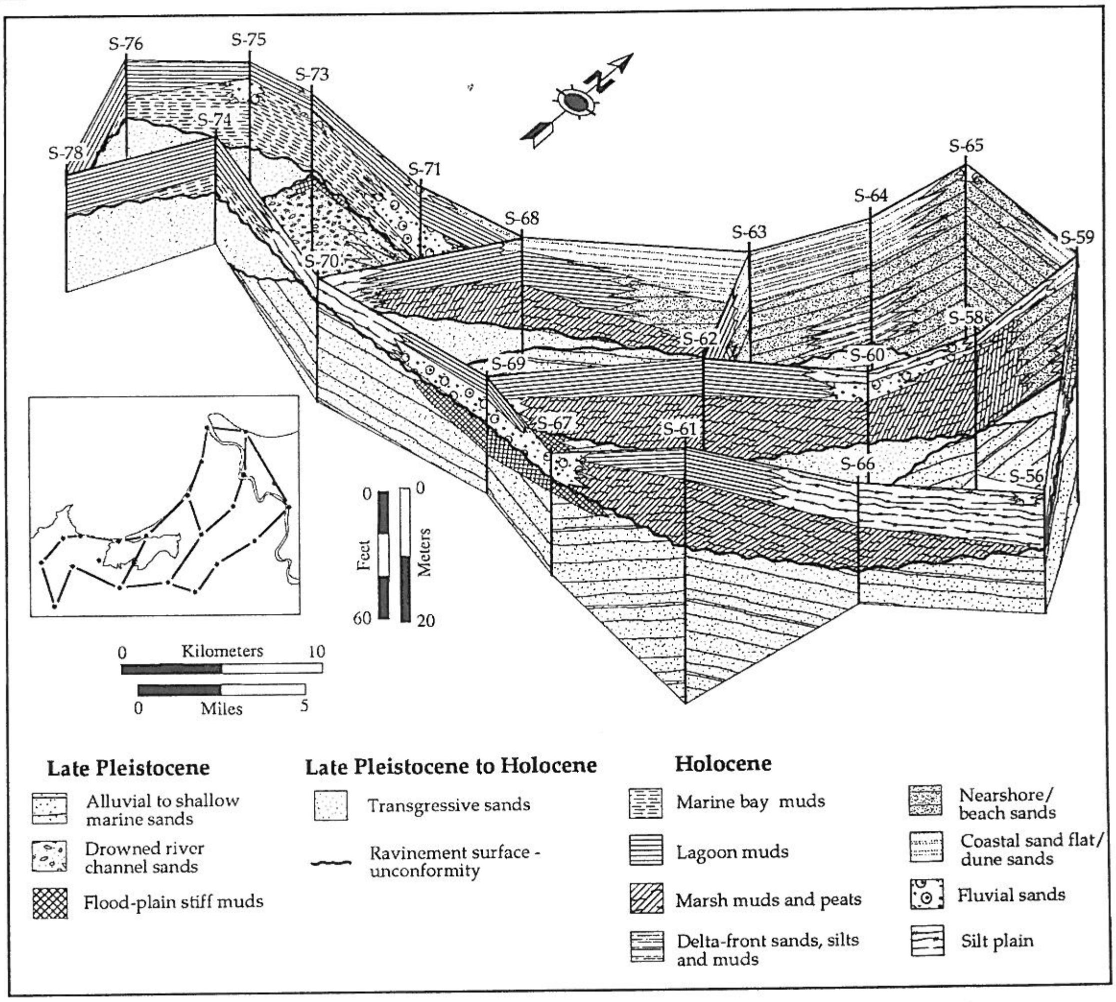

Figure 8. Stratigraphic fence-diagram, compiled on the basis of 20 Smithsonian borings, summarizing late Pleistocene and Holocene lithofacies distributions in time and space.

east of Abu Qir ridge (see core S-73 in Figures 8 and 9A–A′). These coarse sands record the location of the Canopic branch. The presence of the high-relief carbonate ridge (older than 35,000 years BP) positioned just west of S-73 (Figure 2) indicates that this channel was the major westernmost River Nile distributary during the latest Pleistocene.

(3) Late Pleistocene flood-plain stiff muds (~35,000–11,000 years BP) occur locally at or near the top of the Pleistocene sands (Figures 8 and 9A–A′). These muds are interpreted to be overbank deposits which accumulated in localized depressions during seasonal floods.

(4) Late Pleistocene to early Holocene shallow marine transgressive sands occur in the northern part of the study area (Figures 8 and 9A–A′, C–C′); these sands overlie older late Pleistocene alluvial sands and muds. Transgressive sands rapidly pinch out to the south, near the southern margin of the modern Idku lagoon, and indicate the southern limit of the late Pleistocene to early Holocene marine transgression. An unconformity occurs at the base of the transgressive sands and is the result of wave reworking of older, late Pleistocene alluvial deposits as the shoreline retrograded southward.

(5) An unconformity occurs at the top of trans-

© 2001 INIST CNRS. Tous droits de propriété intellectuelle réservés. Reproduction, représentation et diffusion interdites. Loi du 01/07/92. Articles 5, 6 et 7 des CGV.

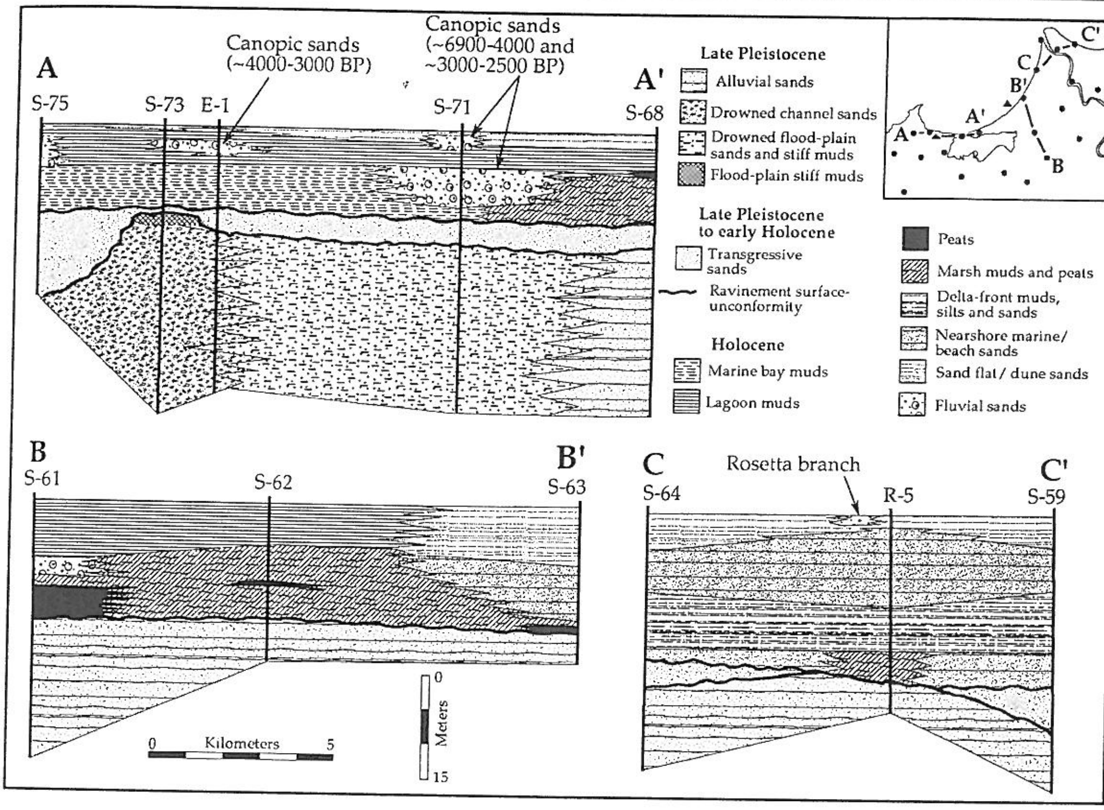

Figure 9. Cross-sections showing late Pleistocene and Holocene lithofacies correlations in three sectors of the study area. Positions of former Canopic and subrecent Bolbitic-Rosetta distributaries are shown.

gressive sands in the northern study area. This hiatus is, in part, a ravinement surface and was caused by shoreface erosion (SWIFT, 1968; NUMMEDAL and SWIFT, 1987) during the Flandrian transgression. Holocene deltaic sediments began to accumulate above the hiatus as the rate of sea-level rise markedly decelerated between ~8,000 to 5,000 years BP. Radiometric dates indicate that onset of Holocene sedimentation above the hiatus occurred at different times within the study area, and may be related to local emergence during the early Holocene (Figure 6A).

(6) Holocene sequences above the unconformity thicken from south to north across the study area (Figures 6 and 8).

(7) No complete Holocene fining-upward (prodelta to delta plain) sequences occur in the study area. Rather, sequences comprise marine bay to lagoon facies in the western sector (Figure 9A–A′), marsh to lagoon facies in the eastern sector (Figures 8 and 9B–B′), and delta-front to nearshore/beach to sand flat/coastal dune facies in the Rosetta promontory sector (Figures 8 and 9C–C′).

(8) Previous studies (ANWAR *et al.*, 1984; EL ASKARY and FRIHY, 1986) indicate that muddy peats (marsh facies) of early Holocene age occur beneath marine deltaic facies in several cores from the Rosetta promontory (Figure 9C–C′). The upward marsh to delta-front transition in the promontory suggests an evolution from early Holocene delta plain to marine deltaic sequence. However, our Rosetta promontory cores do not recover marsh muds beneath the delta-front deposits. We interpret this irregular occurrence of marsh facies to be the result of local littoral erosion of delta plain deposits as the early Holocene sea level rise inundated the former delta plain surface.

(9) Early Holocene (~7,000–5,000 years BP) river channel sands (S-71; Figures 8 and 9A–A′) separate fresh water marsh deposits to the east from time-equivalent open marine bay deposits to the west. We interpret the marsh development

© 2001 INIST CNRS. Tous droits de propriété intellectuelle réservés. Reproduction, représentation et diffusion interdites. Loi du 01/07/92. Articles 5, 6 et 7 des CGV.

in the east to be related to the development of a barrier beach system from sediment transported to the coast by the Canopic channel and then redistributed eastward by littoral currents and winds. This barrier beach system prevented inundation by the sea and subsequent development of marsh. In the western part of the study area, open marine bay conditions prevailed primarily because the Abu Qir ridge promontory deflected eastward-directed littoral currents (see Figure 2, inset) thereby inhibiting barrier beach formation.

(10) Middle and late Holocene lagoon deposits occur throughout the study area, demonstrating that, until recently, coastal wetlands were the predominant ecosystem of the northwestern Nile delta plain environment.

(11) A 46 m long, all-sand core (S-65) was recovered in the northwestern part of the Rosetta promontory (Figure 8). These deposits are interpreted to be river mouth (lower part) and near-shore marine/beach (upper part) facies. The absence of delta-front and marsh facies in the lower portion of this core is interpreted to be the result of erosion associated with river channel migration (see also El Fishawi, 1985).

(12) Sand flat facies make up the upper portions of cores (S-63, S-64, S-68) along the coast to the west of the Rosetta promontory (Figure 8). Radiometric ages indicate that the sand flat deposits are less than 2,000 years old. These sand flats are interpreted to be product of erosion of the Rosetta headland, including some westward littoral transport of eroded sands (see Figure 2, inset), and also deposition entrained by southeastward-directed waves. The sand flat facies thin to the west along the flank of the Rosetta promontory (from S-64, S-68), thus providing evidence for the westward littoral transport of eroded promontory sands.

(13) Holocene fluvial sands interfinger with marine bay, lagoon and marsh deposits (Figures 8 and 9A–A′, B–B′). These sands were deposited by both former Canopic and current Bolbitic-Rosetta River Nile distributaries.

(14) Silt plain facies comprise the upper portions of cores in the western and eastern sectors and are primarily distributed adjacent to fluvial sands (Figure 8). These silty muds were deposited as River Nile overbank deposits during late Holocene annual floods.

DISTRIBUTARY CHANNELS: DEFINITION AND SIGNIFICANCE

During the course of delta evolution, distributaries characteristically migrate and are periodically abandoned (*cf.* Coleman, 1982). Previous Nile delta studies (Toussoun, 1922; Said, 1981; Coutellier and Stanley, 1987; El Fattah and Frihy, 1988; Wunderlich, 1988, 1990; Sestini, 1989; Arbouille and Stanley, 1991; Stanley *et al.*, 1992) have described several former and extant channels which have a complex history of migration and abandonment. In this study, distributary channels are mapped in the subsurface to determine their history of onset, migration and abandonment. Identification of Nile distributary systems helps to define regional geometry and distribution of associated delta plain (lagoon, marsh and silt plain) facies which constitute most of the Holocene section in the study area.

Early descriptions and maps (Arrowsmith, 1807) cited in Toussoun, 1922; UNDP/UNESCO, 1978; Said, 1981; El Askary and Frihy, 1986; El Fattah and Frihy, 1988; Frihy and Komar, 1991; reveal that there were at least seven major Nile distributaries during the past 2,500 years. All were not all active at the same time and, presently, only two remain: the Rosetta and Damietta (Figure 1, inset). Of the seven major early channels, two were located in the study area: the Bolbitic (precursor of the Rosetta) in the east, and the Canopic in the west (Figure 10).

Precise surficial mapping of these former distributaries by satellite remote sensing (Abdel-Kader, 1982) and aerial photography (Frihy, 1988) is ineffective because of lateral channel migration and subsequent development of an extensive irrigation network and intense cultivation. Subsurface analysis of radiocarbon-dated cores is a more reliable method to distinguish the distribution and evolution of these River Nile distributaries.

Bolbitic-Rosetta System

The Rosetta is the larger of the two active River Nile channels which, until recently (prior to closure of the High Aswan Dam and emplacement of irrigation structures in the northwestern delta) carried ~70% of the River Nile water to the coast. It flows northwestward across the eastern part of the study area. Early records, including those of Herodotus (~2,500 years BP), show the Bolbitic (pre-Rosetta) system as a minor canal (Toussoun, 1922; Said, 1981). Subsurface analysis of radiocarbon-dated cores reveals the absence of fluvial sands in the eastern part of the study area during the period ~7,500–3,000 years BP (Figures 8 and 9C–C′) which suggests that the Bolbitic channel system did not exist during that period. Our anal-

© 2001 INIST CNRS. Tous droits de propriété intellectuelle réservés. Reproduction, représentation et diffusion interdites. Loi du 01/07/92. Articles 5, 6 et 7 des CGV.

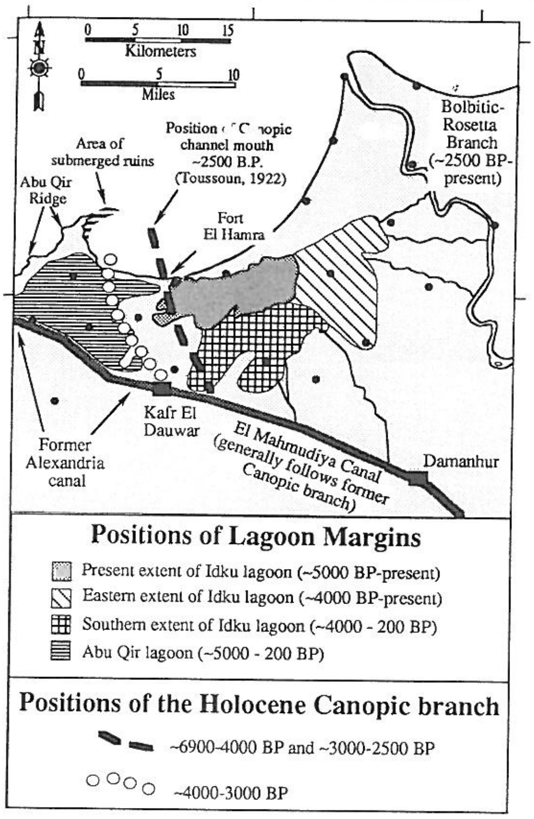

Figure 10. Map of the study area showing the locations of (1) the Canopic channel and (2) Idku and Abu Qir lagoons, and their evolution through time.

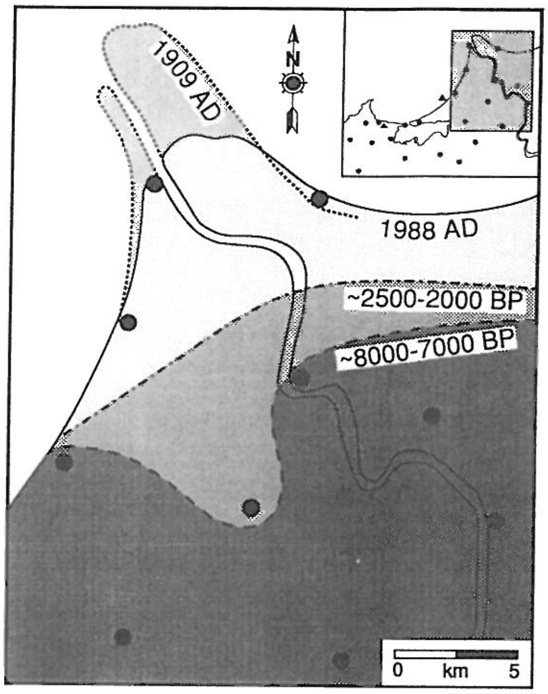

Figure 11. Map showing the change in the configuration of the Rosetta promontory through time, as derived from core analysis. Position of the shoreline from 1909 to 1988 AD is after El-Raey *et al.* (1989).

ysis of radiocarbon-dated lithofacies shows that the Bolbitic-Rosetta has been a major Nile channel for the period ~2,500 years BP to the present. This is confirmed by historical records indicating that the Rosetta-Bolbitic channel system was excavated by man as early as 2,500 years BP (*cf.* SAID, 1981).

The development of the Bolbitic-Rosetta channel system is demonstrated by mapping the location of the paleoshoreline through time (Figure 11). From ~8,000 to 2,000 years BP, before the Bolbitic-Rosetta channel became significant, the coastline prograded slowly, at an average rate of 0.5 m/yr (0.5 km/1,000 yr). Then from ~2,000 years BP to 1908 AD the Rosetta developed into a major Nile distributary (SMITH and ABDEL-KADER, 1988); large volumes of sediments were transported to the coast by the Rosetta branch which resulted in rapid shoreline progradation at an average rate of 6 m/yr (6 km/1,000 yr) and formation of a large headland region. Rosetta promontory sediments are as thick as 35 m (Figure 12), and form a triangular-shaped headland. Since its closure in 1964, the Aswan High Dam and Lake Nasser have trapped virtually all River Nile sediments. As a consequence, River Nile sediments are no longer being delivered to the coast by the Rosetta channel, and the northern part of the promontory has been rapidly eroding (UNDP/UNESCO, 1978; SMITH and ABDEL-KADER, 1988; EL-FISHAWI and BADR, 1989; EL-RAEY *et al.*, 1989; BLODGET *et al.*, 1991; see Figure 3A). The average erosion rate is 63 m per year; locally, however, erosion rates to 275 m per year have been determined (SMITH and ABDEL-KADER 1988).

Canopic System

The Canopic branch was the westernmost of the seven ancient Nile channels. Many authors have indicated that the Canopic channel was a principal Nile channel between ~2,500 and 2,000 years BP, and for a time was the only channel

© 2001 INIST CNRS. Tous droits de propriété intellectuelle réservés. Reproduction, représentation et diffusion interdites. Loi du 01/07/92. Articles 5, 6 et 7 des CGV.

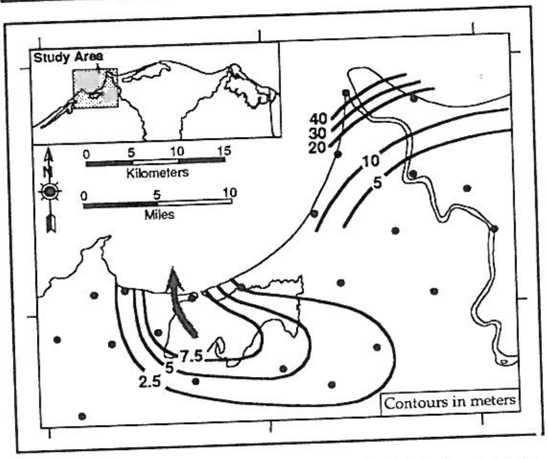

Figure 12. Isopachous map of Holocene fluvial-derived sands, compiled on the basis of petrographic analysis of core sections. The two distinct sand bodies are related to the Bolbitic-Rosetta channel (in the east) and the Canopic branch (in the west).

navigable from the Mediterranean coast to Cairo and Memphis (Toussoun, 1922). North of Cairo, the Canopic branch flowed generally north-northwestward across the delta plain until Damanhur city (Figure 10), from which it flowed in a more west-northwesterly direction to the Mediterranean Sea. Several early authors (*e.g.*, Herodotus and Pliny, *in* Toussoun, 1922) report that the mouth of the Canopic was about 6 km north-northwest of Fort El Hamra (Figure 10), which is presently on the coast west of Maadia (Figure 2). The Canopic channel waned in importance and eventually silted, following re-excavation of the Bolbitic canal.

Lithofacies evidence clearly shows that the Canopic branch was a major Nile distributary for the period ~7,000–4,000 years BP, and then declined in very recent time; its presence was still noted two centuries ago (Arrowsmith, 1802, 1807). During its early history, this distributary transported large volumes of sediment to the western Abu Qir Bay region. There is little geomorphic evidence for a Canopic promontory along the coast, but the form and size of the Rosetta Cone on the continental shelf northwest of Rosetta (UNDP/UNESCO, 1978) suggest that this conspicuous wedge of late Quaternary sediments may have been in part deposited by materials transported via the Canopic channel. Cores S-63 and E-2, located along the eastern Abu Qir Bay coastline (Figures 1 and 8), contain thick (>18 m) sections of sand of Holocene age which are interpreted to be associated with the Canopic promontory. This latter feature would now be submerged offshore north of Idku lagoon, probably in the northwest part of Abu Qir Bay. It is of special note that on some bathymetric charts (UNDP/UNESCO, 1978, p.82) there is evidence of a north-trending channel-like depression extending from near the coast to about 10 km north of Fort El Hamra (to a depth of about 20 m). Toussoun (1934) suggested that this linear trough was the northward extension of the Canopic branch.

It is postulated that sands forming the coastal flats and dunes along the western flank of the Rosetta promontory are derived, at least in part, from the once partially emerged promontory at the mouth of the Canopic branch. The distribution of surficial sandy sediments in Abu Qir Bay provides evidence for eastward-transported terrigenous sands (*cf.* Summerhays *et al.*, 1978, their Figure 6); we suggest that some of these sediments were eroded from the former promontory by littoral and wind-driven wave currents. An offshore survey in Abu Qir Bay involving long cores and high-resolution seismic profiling is required to clearly determine the location and extent of the former Canopic promontory.

We determine the position of the former Canopic branch on the lower delta plain through time by interpretation of subsurface lithofacies data derived from core analysis (Figure 10) and by examintion of topographic maps (Arrowsmith, 1802, 1807; Toussoun, 1922; U.S. Defense Mapping Agency, 1977, 1981; Said, 1981). It is of note that the El Mahmudiya canal, a most important man-made drainage in the present western Nile delta, trends west-northwest from Damanhur through Kafr El Dauwar to Alexandria (Figure 10). Ancient maps show that the course of the El Mahmudiya canal between Damanhur and Kafr El Dauwar followed, for the most part, the former Canopic branch (Figure 10). The segment of the present El Mahmudiya canal between Kafr El Dauwar and Alexandria parallels the former Alexandria canal (Said, 1981).

The location of the Canopic branch north of the Kafr El Dauwar varies on different early maps (Figure 10). Some depict the Canopic flowing across the western portion of Idku lagoon toward the Mediterranean Sea (El Fattah and Frihy, 1988); a second view proposes flow along the western margin of Idku lagoon toward the sea (*e.g.* Frihy and Komar, 1991); and a third interpretation shows that the branch lay further to the

© 2001 INIST CNRS. Tous droits de propriété intellectuelle réservés. Reproduction, représentation et diffusion interdites. Loi du 01/07/92. Articles 5, 6 et 7 des CGV.

west, *i.e.* flowed northward just east of Abu Qir ridge (*e.g.* EL-FAYOUMY *et al.*, 1975). Most authors do not specify the time-span of these various courses of the Canopic channel. The present study, which is based primarily on radiocarbon-dated cores, demonstrates that the Canopic branch has in fact had a complex history of channel migration through time.

Subsurface core profile transects (Figures 8 and 9) and an isopachous map of fluvial and fluvially-derived coastal sands of Holocene age (Figure 12) provide new information to interpret the origin of presently buried channels. These data highlight two subsurface channel systems in the study area: an eastern one which helps define the trend of the Rosetta channel, and a western system which encompasses the trend of the buried Canopic channels. The isopachous map indicates that the Canopic channel during most of the Holocene flowed west-northwestward to Idku lagoon, and at that point veered toward a more northward direction (*i.e.* along the western margin of the present-day lagoon and just to the west of Maadia). This trend is also suggested by mapping along the Abu Qir coastline the distribution of coarse sands (EL ASKARY and FRIHY, 1986; FRIHY *et al.*, 1988) and of heavy minerals (EL-BOUSEILY and FRIHY, 1984; EL FATTAH and FRIHY, 1988). However, mapping of radiocarbon-dated subsurface facies (Figures 8 and 9A–A′) reveals that, over time, the northern portion of the Canopic branch actually migrated across this area (Figure 10). During the period ~6,900–4,000 years BP, the Canopic flowed along the western margin of Idku lagoon. Then from about 4,000 to 3,000 years BP the channel migrated westward to just east of present-day Abu Qir carbonate ridge (Figure 10). Finally, during the period ~3,000–2,500 years BP, the Canopic shifted eastward back to its former position along the western margin of Idku lagoon. Although flow continued to decrease, the channel has remained in this latter position until the recent past.

It is of interest that lithofacies analysis of pre-Holocene core sections also records the presence of a major river channel system in the study area during late Pleistocene (Figure 9, 9A–A′). The location of this late Pleistocene channel is coincident with the Canopic branch (at ~4,000–3,000 years BP) which flowed just to the east of Abu Qir ridge. We interpret this well-defined Pleistocene channel system (consisting of coarse, highly stained sands with interbedded thin stiff muds) to be the precursor of the Canopic branch. There is no evidence to suggest that the course of either the late Pleistocene or Holocene channel systems in the northwestern Nile delta are fault controlled (SAID, 1981; NEEV *et al.*, 1985; SESTINI, 1989); however, some degree of deep-seated tectonic control cannot be ruled out.

WETLAND LOSS: THE ROLE OF NATURAL PROCESSES AND MAN

Lagoons are an integral part of the northern Nile coastal plain. Presently, Manzala, Burullus, Idku and Maryut lagoons extend along about half of the total northern Nile coastal region. Subsurface data and early maps show that lagoons and marshes occupied considerably larger areas of the lower Nile delta plain-coastal region during much of the Holocene than they do today (ARROWSMITH, 1802, 1807; DU BOIS-AYME, 1813; SAID, 1981; COUTELLIER and STANLEY, 1987; ARBOUILLE and STANLEY, 1991; STANLEY *et al.*, 1992). During the past two centuries, there has been accelerated loss of lagoons and associated marsh areas. In the study area, Idku lagoon has undergone substantial subsurface area loss, and Abu Qir lagoon, prominent on maps two centuries ago, has been completely drained. Further reduction of remaining wetlands, vital but delicate plant-rich habitats for wildlife, is of serious concern for they are an important source of fish and other aquacultural products at a time when Egypt's population is growing at record rate. In spite of their importance, these lagoons are being very rapidly drained and reclaimed by man, primarily for agricultural use, and what remains unfortunately is being polluted with municipal sewage and industrial waste (WARNE and STANLEY, 1991). Herein, we briefly summarize (on the basis of core lithofacies analysis) the Holocene evolution and demise of the Idku and former Abu Qir wetlands.

Much of the Idku lagoon region was occupied by fresh water marsh during the period ~7,500–5,000 years BP; at that time, 8 to 11 m of vegetal-rich layers, peats, and peaty muds accumulated. Brackish water lagoons then prevailed as early as ~5,000 years BP, during which 4–5 m of organic-rich muds accumulated. We postulate that from ~7,500–5,000 years BP, eastward-directed littoral currents resulted in linear sand barriers which formed to the north of the present coastline; this barrier beach system is believed to have been extensive, for it prevented marine inundation into the Idku area and allowed fresh water marsh con-

© 2001 INIST CNRS. Tous droits de propriété intellectuelle réservés. Reproduction, représentation et diffusion interdites. Loi du 01/07/92. Articles 5, 6 et 7 des CGV.

ditions to prevail. Then at about ~5,000 years BP, as sea level continued to rise, the barrier system was breached by the sea and fresh water marshes gave way to brackish water lagoons. From ~5,000–2,500 years BP, Idku lagoon was much larger than today, extending to as much as 15 km south of the present coastline, and 20 km to the east from the Maadia outlet (Figures 2 and 10). At that time, the Canopic channel flowed along the western border of Idku lagoon and separated it from the former Abu Qir lagoon to the west. Our subsurface analyses and examination of early maps indicate that during the past 2,000 years Idku lagoon has shrunk from ~375 km² to ~120 km² (Figure 10). On the basis of a map compiled by Arrowsmith (1807), we find that Idku lagoon has been reduced to less than half of its surface area (~200 km²) during the past 200 years.

Moreover, early maps and documents indicate that a large (~130 km²) lagoon was located southeast of Abu Qir ridge and west of Idku (Figure 10). This former lagoon (Figure 3F), known as Abu Qir Lake (Arrowsmith, 1802, 1807; Toussoon, 1922), has now been entirely converted into irrigated farmland. Like Idku, brackish water conditions began in the Abu Qir lagoon area ~5,000 years BP; unlike Idku, however, Abu Qir lagoon evolved from an open marine bay rather than from a marsh (Figures 4, 8, 9). We find no firm evidence to indicate that the Abu Qir and Idku lagoons were connected. Rather, it would appear that levee and overbank silts of the Canopic channel system separated these two brackish water bodies for much of the Holocene.

The shrinkage and disappearance of Nile delta lagoons can, in general, be attributed to two factors: nature and man. In the study region, loss of Idku and Abu Qir lagoon surface area can be attributed almost entirely to human activity. For example, Idku and Abu Qir wetland loss has been brought about because of much reduced flow through Canopic channel which formerly supplied fresh water to these brackish water bodies; it is recalled that disappearance of the Canopic channel is primarily the result of excavation of the Bolbitic-Rosetta channel to the east. The disappearance of Abu Qir lagoon is also the result of blockage of its outlet by man (El-Fayoumy *et al.*, 1975) at El Tarh (Figure 2). In summary, both Idku and Abu Qir wetland loss are attributed to decreased freshwater flow to the coast and land reclamation projects, both the result of man's increased intervention (Waterbury, 1979).

PALEOGEOGRAPHICAL EVOLUTION AND CONCLUSIONS

Subsurface distributions of late Pleistocene to Holocene lithofacies and evolution of sedimentary environments in the northern Nile delta between Rosetta branch and Alexandria have been defined on the basis of petrological, faunal, floral and chronostratigraphic analyses of radiocarbon-dated cores. Lithofacies and paleoenvironment distributions are made, taking into account the effects of major natural controlling factors: eustatic, subsidence and neotectonics, paleoclimate and transport processes.

This analysis makes it possible to better understand the unique Holocene subsurface attributes of the study area: (1) thin sections in the southern and western sectors; (2) previously undescribed marine bay muds in the western sector; (3) well-developed sequences of marsh peats in the eastern sector (thickest in the entire northern delta); (4) thick fluvially-derived sand sections at the Rosetta promontory; and (5) thick barrier beach sand sequences in the northern sector (Figures 4, 8, 9).

Mapping of subsurface lithofacies and paleoenvironment distributions are also used to more precisely interpret the unique geomorphic attributes of the study area: (1) a distinctive coastline configuration comprising the Rosetta promontory in the northeast, broadly concave Abu Qir Bay coastline in the center, and Abu Qir ridge promontory in the west; (2) Idku and former Abu Qir lagoons; (3) kôms to the south and southeast of Idku lagoon; and (4) the coastal sand flats and dune fields on the western flank of Rosetta promontory.

A synthesis of northern Nile delta evolution between Rosetta promontory and Alexandria during the past ~35,000 years is summarized below in a series of paleogeographic maps (Figure 13). These maps, which consider the area during six time periods, integrate lithofacies distributions, the factors which control sediment distribution, and geomorphic features.

From ~35,000 to 11,000 years BP (Figure 13A), the northern delta coast migrated from its near-present position during the last Pleistocene sea-level high-stand, to as much as 50 km to the north (near the shelfbreak) during the last Pleistocene low-stand (~20,000–18,000 years BP), and then southward (landward) to what is now the mid-shelf. During this time-span, the study area was a subaerially exposed, gently seaward-dipping, sandy alluvial plain with local and ephemeral flood

© 2001 INIST CNRS. Tous droits de propriété intellectuelle réservés. Reproduction, représentation et diffusion interdites. Loi du 01/07/92. Articles 5, 6 et 7 des CGV.

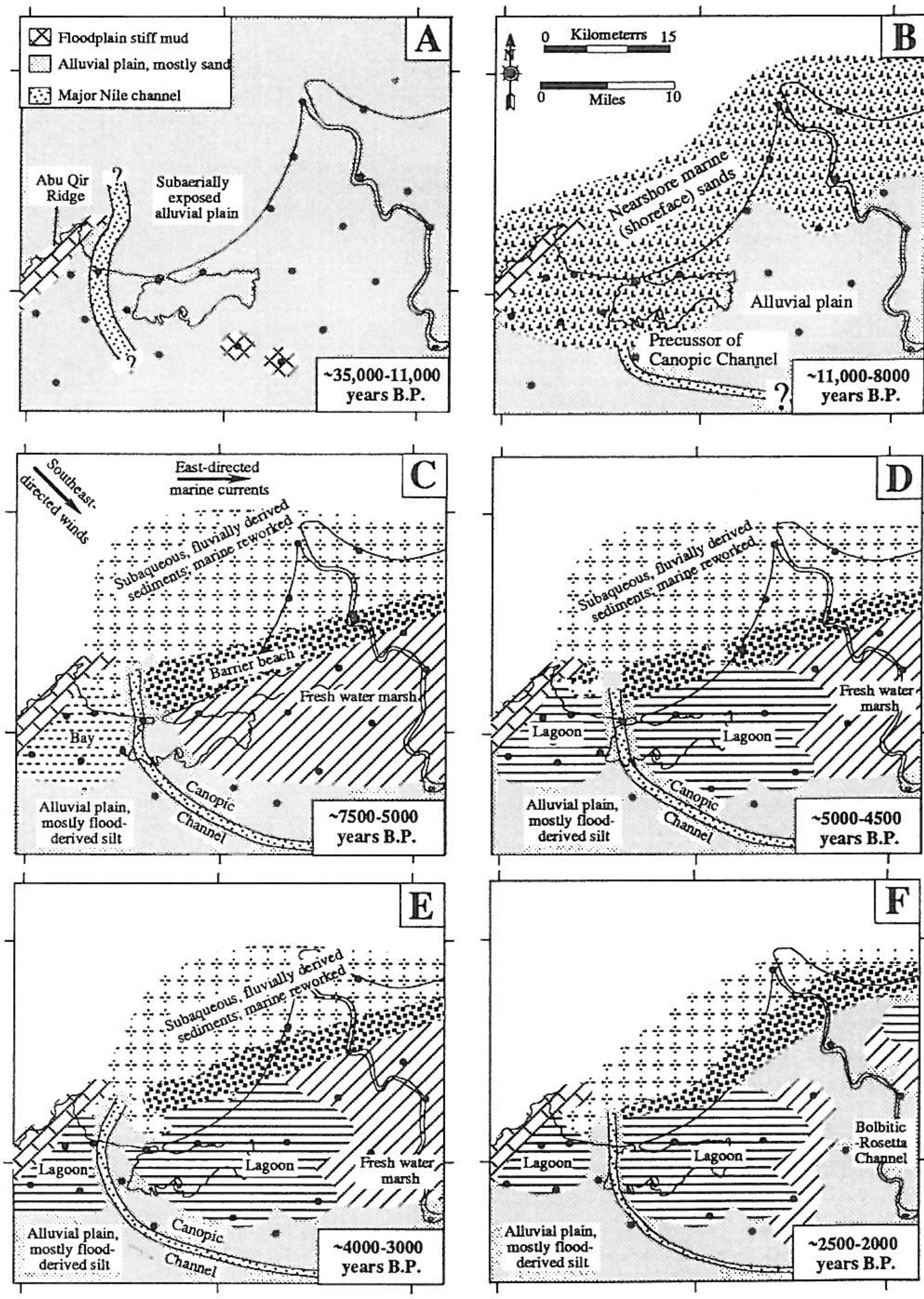

Figure 13. Series of time-slice paleogeographic maps showing the late Pleistocene to Recent evolution of the northwestern Nile delta between Rosetta promontory and Alexandria (explanation in text).

© 2001 INIST CNRS. Tous droits de propriété intellectuelle réservés. Reproduction, représentation et diffusion interdites. Loi du 01/07/92. Articles 5, 6 et 7 des CGV.

plain depressions. A NNW-trending major, primarily braided, river channel (pre-Canopic) flowed across what is now the northwest portion of the delta to the present-day shelf edge (*cf.* Maldonado and Stanley, 1979). This river channel was periodically inundated by brackish water during intermittent eustatic sea-level rises. Large pebbles in flood-plain muds (S-67, S-69) record the large capacity of this ancestral River Nile channel. Flood-plain muds were deposited in localized shallow depressions and playas. Gypsum and calcareous nodules in these stiff muds record repeated drying and wetting conditions in a generally arid climate. Continuous river channel switching and migration during this period eroded most flood-plain muds which had earlier accumulated in the study area.

From ~11,000 to 8,000 years BP (Figure 13B), the coast migrated southward (landward) from the mid-shelf as sea level rose rapidly, resulting in deposition of nearshore marine (shoreface) and beach transgressive sands. The late Pleistocene-early Holocene transgressive sand unit is the product of reworked older Pleistocene deposits. An unconformity separates the relatively undisturbed late Pleistocene deposits from the overlying, reworked late Pleistocene-early Holocene transgressive sands. Shoreface erosion, associated with the continued rapid rise in sea level, resulted in ravinement surfaces at the top of the transgressive sand. Local emergence resulted in prolonged periods of nondeposition and erosion at this ravinement surface, especially in the south and west of the study area. Available subsurface data does not provide information about River Nile channels in the study area or the emerged alluvial plain to the south during this period.

By ~7,500 years BP, the rate of sea-level rise had begun to decelerate, so that by ~6,000–5,000 years BP (Figure 13C) accumulation of Holocene Nile delta sediments was well underway. In the study area, the shoreline prograded only a few km to the north from ~7,500–5,000 years BP. The climate was more humid than at present and seasonal floods likely resulted in high fluvial discharge. The Canopic, the major distributary in the northwestern Nile delta plain flowed northwestward across the south-central study area and then northward along the western margin of Idku lagoon and into southwest Abu Qir bay. The channel transported large volumes of sands (especially during floods) which accumulated in the Abu Qir bay region, where it probably formed a promontory at its mouth. Strong eastward-directed littoral drift and southeastward-directed wave currents redistributed these river promontory sands to the east and southeast in the Rosetta promontory region. These marine reworked sands accumulated as barrier islands and spits and acted as a barrier which prevented inundation of the sea into the eastern study area. The combination of the barrier beach system and influx of large volumes of fresh water by the Canopic channel resulted in widespread development of marshes in the eastern part of the study area. In contrast, marine bay conditions prevailed in the western part of the study area during this time; the Abu Qir ridge promontory deflected the eastward-directed marine wave and littoral currents which prevented isolation (cut-off by spits and barrier islands) of the bay from the open sea.

By ~5,000–4,500 years BP (Figure 13D), the rate of sea-level rise continued to decelerate and the climate became more arid. The Canopic channel continued to flow along the western margin of the present-day Idku lagoon. Although the Rosetta promontory sector continued to sustain a barrier island system, rising sea level and the diminished supply of river-derived sediment resulted in local breaching of the sand barrier system. Some of these outlets became perennial channels between the coastal lagoons and the sea which brought about a widespread change from fresh water marsh to brackish water lagoon conditions in the east-central part of the study area. This large brackish water body became the predecessor of the modern Idku lagoon. Fresh water marsh conditions persisted along the southern and eastern parts of the study area. In the western part of the study area, fluvial sediments, reworked by marine waves and currents, formed spits along the northern end of the open marine bay. These linear coastal sand bodies restricted marine influence and resulted in widespread, brackish water lagoon conditions in the western sector. This brackish water body was the predecessor of the Abu Qir lagoon.

At ~4,000–3,000 years BP, sea level steadily rose to ~4–3 m below its present stand; the climate continued to become more arid. The coastline was almost at its present position in central and western Abu Qir Bay. During this time, the Canopic had migrated to the west where it flowed along the eastern margin of the Abu Qir lagoon, and just east of Abu Qir ridge. The course of the Canopic channel (Figure 13E) at this time appears

© 2001 INIST CNRS. Tous droits de propriété intellectuelle réservés. Reproduction, représentation et diffusion interdites. Loi du 01/07/92. Articles 5, 6 et 7 des CGV.

to be coincident with the trace of the late Pleistocene river channel (Figure 13A). Delta-front (or perhaps inner shelf) sands, silts and muds were deposited in what is now the Rosetta promontory sector north of the barrier beach system; these facies may have accumulated at a time of reduced sediment input by the Canopic channel.

By ~2,500–2,000 years BP, the Canopic branch was diminishing as a significant Nile distributary, and its demise was apparently accelerated by artificial excavation of the Bolbitic-Rosetta branch (*cf.* SAID, 1981). Continuous channel excavation from ~2,000 years BP lead to the Bolbitic-Rosetta becoming the principal Nile distributary in this region. As a result, the shoreline at the mouth of the Rosetta began to receive large volumes of sediment so that it prograded rapidly seaward forming a triangular promontory (Figures 11, 12, 13F). This large promontory resulted in refraction of eastward-directed littoral currents and formation of a counter-clockwise eddy on the western side of the promontory (Figure 2, inset). Abu Qir and Idku lagoons diminished in size as the volume of fresh water carried by the Canopic channel decreased, and man drained and infilled these wetland regions for agriculture. Due to artificial excavation, the Rosetta channel became the principal River Nile channel, delivering large volumes of sand to its promontory headland. These sediments were redistributed to both sides of the promontory by eastward littoral currents, counter clockwise westward-directed eddy currents, and eolian transport. These littorally transported sediments formed broad sand flats and strand plains along the flanks of the Rosetta promontory.

Since ~2,000 years BP the Canopic branch has been converted into an artificial canal and drain system. Curtailment of influx of fresh water into the region has resulted in the disappearance (within the past 200 years) of Abu Qir lagoon, and the reduction of Idku lagoon to ~30% of it former size. Most of the former lagoon surfaces are now cultivated. The Rosetta channel transported 70% of River Nile water and sediments until the beginning of this century. The large volumes of river-borne sediments carried to the coast by the Rosetta branch resulted in seaward progradation of the Rosetta promontory by as much as 17.5 km (Figure 11). During this century, dams in Upper Egypt and the barrage-irrigation network in the delta have effectively cut off the sediment supply to the lower delta plain and coastal region. In response, the Rosetta promontory has retrograded more than 5 km in the past 80 years (Figure 11).

It is likely that Idku lagoon will continue to be reduced, and unless stringent measures are taken most of this wetland region will likely disappear in the next century. Moreover, the Rosetta promontory remains susceptible to erosion. Although its northernmost sector is protected by recently-constructed sea wall structures (Figure 3A), margins of the Rosetta promontory will continue to retrograde southward (Figure 3B–D). Lateral displacement of eroded sand is expected to result in expansion of sand flats and dune fields on the western flank of the promontory (Figure 2). Although our data base records generally modest subsidence rates in this region, even a modest rise in sea level (*cf.* TITUS, 1986), would likely result in widespread shoreline retrogradation and marine inundation of low-lying areas, including former lagoons, south of Abu Qir bay. Marine inundation will be accelerated because Nile sediments are no longer being delivered to the coast. Increased salinization of shallow groundwater will, in turn, negatively affect agricultural production in the coastal region.

ACKNOWLEDGEMENTS

We thank Prof. A. Bassiouni, Dean, Faculty of Sciences, Ain Shams University, Cairo, and Dr. B. Issawi, Under Secretary for State, Cairo, for facilitating field work and providing strong support for the Nile Delta Project. Appreciation is expressed to Eng. A. Madi, Mr. M. Hamzawi and the two drill crew teams of MISR Raymond Foundations in Ismailia for their efficient drilling of the borings. Drs. H.L. Howa and D. Arbouille contributed much to the petrologic study of some borings used in the study. Dr. F. Hamza and Messrs. S. Miller and W. Boykins assisted with core sample analyses at the Sedimentology Laboratory-NMNH. Dr. M.P. Bernasconi identified and interpreted the molluscan assemblages in selected samples in two cores. The manuscript was reviewed by Drs. M. Kontrovitz and J.-L. Loizeau. Financial support was generously provided by grants from the Smithsonian Scholarly Studies Program, National Geographic Society, Director's Office at the U.S. National Museum of Natural History, Smithsonian Office of Fellowships and Grants, Smithsonian Assistant Secretary for Research, and Elf-Aquitaine (Washington).

© 2001 INIST CNRS. Tous droits de propriété intellectuelle réservés. Reproduction, représentation et diffusion interdites. Loi du 01/07/92. Articles 5, 6 et 7 des CGV.

LITERATURE CITED

ABDEL-KADER, A., 1982. Landsat analysis of the Nile Delta, Egypt. M.Sc. Thesis, Univ. of Delaware, Newark, Delaware, 260p.

ABDEL WAHAB, H.S. and STANLEY, D.J., 1991. Clay mineralogy and the recent evolution of the north-central Nile delta, Egypt. *Journal of Coastal Research*, 7, 317–329.

ABU-ZEID, M.M. and STANLEY, D.J., 1990. Temporal and spatial distribution of clay minerals in Late Quaternary deposits of the Nile delta, Egypt. *Journal of Coastal Research*, 6, 677–698.

ADAMSON, D.A.; GASSE, F.; STREET, F.A., and WILLIAMS, M.A., 1980. Late Quaternary history of the Nile. *Nature*, 288, 50–55.

ANWAR, Y.M.; EL ASKARY, M.A., and FRIHY, O.E., 1984. Reconstruction of sedimentary environments of Rosetta and Damietta promontories in Egypt, based on textural analysis. *Journal of African Earth Sciences*, 2, 17–29.

ARBOUILLE, D. and STANLEY, D.J., 1991. Late Quaternary evolution of the Burullus lagoon region, north-central Nile delta, Egypt. *Marine Geology*, 99, 45–66.

ARROWSMITH, A., 1802. *Plan of the Operations of the British and Ottoman Forces in Egypt*. London (map, 1 sheet).

ARROWSMITH, A., 1807. *A Map of Lower Egypt from Various Surveys Communicated by Major Bryce and Other Officers*. London (map, 1 sheet).

ATTIA, M.I., 1954. *Deposits in the Nile Valley and the Delta*. Cairo: Geological Survey of Egypt, 356p.

BELL, B., 1970. The oldest records of Nile floods. *Geographic Journal*, 136, 569–573.

BERNASCONI, M.P.; STANLEY, D.J., and DI GERONIMO, I., 1991. Molluscan faunas and paleobathymetry of the Holocene sequences in the Nile delta, Egypt. *Marine Geology*, 99, 29–43.

BLODGET, H.W.; TAYLOR, P.T., and ROARK, J.H., 1991. Shoreline changes along the Rosetta-Nile promontory: Monitoring with satellite observations. *Marine Geology*, 99, 67–77.

BROUSSARD, M.L. (ed.), 1975. *Deltas, Models for Exploration*. Houston, Texas: Houston Geological Society, 555p.

BUTZER, K.W., 1960. On the Pleistocene shore lines of Arabs' Gulf, Egypt. *Journal of Geology*, 68, 626–637.

BUTZER, K.W., 1976. *Early Hydraulic Civilization in Egypt*. Chigaco Illinois: University Chicago Press, 134p.

CHEN, Z. and YANG, W., 1991. Quaternary evolution of paleogeography and paleoenvironment of the Yangtze estuarine region. *Journal of Geophysica Sinica* (in press).

COLEMAN, J.M., 1982. *Deltas: Processes of Deposition and Models for Exploration* (2nd Edition). Boston, Massachusetts: International Human Resources Development Corp., 124p.

COLEMAN, J.M.; ROBERTS, H.H.; MURRAY, S.P., and SALAMA, M., 1981. Morphology and dynamic sedimentology of the eastern Nile delta shelf. *Marine Geology*, 42, 301–312.

COLLINSON, J.D., 1986. Alluvial sediments. *In:* READING H.G. (ed.), *Sedimentary Environments and Facies*. Boston, Massachusetts: Blackwell, pp. 20–62.

COUTELLIER, V. and STANLEY, D.J., 1987. Late Quaternary stratigraphy and paleogeography of the eastern Nile delta, Egypt. *Marine Geology*, 77, 257–275.

CURRAY, J.R., 1965. Late Quaternary history, continental shelves of the United States. *In:* WRIGHT, H.E., Jr. and FREY D.G. (eds.), *The Quaternary of the United States*. Princeton, New Jersey: Princeton Univ. Press, pp. 723–735.

DI GERONIMO, I. and ROBBA, E., 1976. Metodologie qualitative e quantitative per lo studio delle biocenosi e delle paleocomunita marine bentoniche. *C.N.R. Gruppo Paleobenthos, Rapporto de Lavoro*, n. 1, 1–35.

DU BOIS-AYMÉ, M., 1813. Mémoire sur les anciennes branches du Nil et ses embouchures dans la mer. *Description de l'Egypte, Antiquités, Mémoires. I*, pp. 277–290.

EL ASKARY, M.A. and FRIHY, O.E., 1986. Depositional phases of Rosetta and Damietta promontories on the Nile delta coast. *Journal of African Earth Sciences*, 5, 627–633.

EL-BOUSEILY, A.M. and FRIHY, O.E., 1984. Textural and mineralogical evidence denoting the position of the mouth of the old Canopic Nile branch on the Mediterranean coast, Egypt. *Journal of African Earth Sciences*, 2, 103–107.

EL DIN, S.S.H., 1977. Effect of the High Aswan Dam on the Nile flood and on estuarine and coastal circulation along the Mediterranean Egyptian coast. *Limnology and Oceanography*, 22, 194–207.

EL FATTAH, T.A. and FRIHY, O.E., 1988. Magnetic indications of the position of the mouth of the old Canopic branch on the northwestern Nile delta of Egypt. *Journal of Coastal Research*, 4, 483–488.

EL-FAYOUMY, I.F.; EL SHAZLI, M.M., and HAMMAD, F.A., 1975. Geomorphology of the coastal area between Abu Qir and Rasheed (Northwest of the Nile Delta, E.A.R.). Cairo, Egypt: *Faculty of Science, Cairo University Press*, pp. 135–147.

EL-FISHAWI, N.M., 1985. Textural characteristics of the Nile delta coastal sands: An application in reconstructing the depositional environments. *Acta Mineralogica-Petrographica, Szeged*, 27, 71–88.

EL-FISHAWI, N.M. and BADR, A.A., 1989. Volumetric changes of nearshore sediments between Rosetta and Burullus, Egypt. *INQUA Commission on Quaternary Shoreline Newsletter*, 11, 39–42.

EL-FISHAWI, N.M. and EL ASKARY, M.A., 1981. Characteristic features of coastal sand dunes along Burullus-Gamasa stretch, Egypt. *Acta Mineralogica-Petrographica, Szeged*, 25, 63–76.

EL-FISHAWI, N.M. and FANOS, A.M., 1989. Prediction of sea level rise by 2100, Nile Delta coast. *INQUA Commission on Quaternary Shorelines Newsletter*, 11, 43–47.

EL-RAEY, M.; NASU, S., and FRIHY, O., 1989. National assessment of the impact of greenhouse induced sea-level rise on the northern coastal regions of Egypt. *Report to the University of Maryland at College Park, Maryland*, 11p.

EL SOKKARY, I.H. and MULLER, G., 1989. Contamination of the terrestrial ecosystem by mercury around the industrial complex center of el Max, western area of Alexandria. *In:* VERNET J.-P. (ed.), *International*

© 2001 INIST CNRS. Tous droits de propriété intellectuelle réservés. Reproduction, représentation et diffusion interdites. Loi du 01/07/92. Articles 5, 6 et 7 des CGV.

Conference: Heavy Metals in the Environment, 2, Geneva, Switzerland: CEP Consultants Ltd., pp. 321–324.

El-Wakeel, S.K.; Abdou, H.F., and Wahby, S.B., 1970. Foraminifera from bottom sediments of Lake Maryut and Lake Manzalah, Egypt. *Bulletin of the Institute of Oceanography and Fisheries*, 1, 427–448.

El-Wakeel, S.K. and El-Sayed, M., 1978. The texture, mineralogy and chemistry of bottom sediments and beach sands from the Alexandria region, Egypt. *Marine Geology*, 27, 137–160.

Emery, K.O.; Aubrey, D.G., and Goldsmith, V., 1988. Coastal neo-tectonics of the Mediterranean from tide-gauge records. *Marine Geology*, 81, 41–52.

Fairbanks, R.G., 1989. A 17,000-year glacio-eustatic sea level record: Influence of glacial melting rates on the younger Dryas event and deep-ocean circulation. *Nature*, 342, 637–642.

Foucault, A. and Stanley, D.J., 1989. Late Quaternary paleoclimatic oscillations in East Africa recorded by heavy minerals in the Nile Delta. *Nature*, 339, 44–46.

Fourtau, R., 1896. Les puits artésiens et les puits forés en Egypte. *Bulletin de l'Institut d'Egypte*, 7(3), 239–255.

Frihy, O.E., 1988. Nile Delta shoreline changes: Aerial photographic study of a 28-year period. *Journal of Coastal Research*, 4, 597–606.

Frihy, O.E.; El Fishawi, M.M., and El Askary, M.A., 1988. Geomorphological features of the Nile delta coastal plain: A review. *Acta Adriatica*, 29, 51–65.

Frihy, O.E. and Komar, P.O., 1991. Patterns of beach-sand sorting and shoreline erosion on the Nile delta. *Journal of Sedimentary Petrology*, 61, 544–550.

Frihy, O.E. and Stanley, D.J., 1988. Texture and coarse fraction composition of Nile Delta deposits: Facies analysis and stratigraphic correlation. *Journal of African Earth Sciences*, 7, 237–255.

Gustavson, T.C., 1991. Buried vertisols in lucustrine facies of the Pliocene Fort Hancock Formation, Hueco, West Texas and Chihuahua, Mexico. *Geological Society of American Bulletin*, 103, 448–460.

Hassan, F.A., 1981. Historical Nile floods and their implications for climatic change. *Science*, 212, 1142–1145.

Hayes, M.O., 1979. Barrier island morphology as a function of tidal and wave regime. *In:* Leatherman, S.P. (ed.), *Barrier Islands from the Gulf of St. Lawrence to the Gulf of Mexico.* New York: Academic, pp. 1–28.

Holeman, J.N., 1968. The sediment yield of major rivers of the world. *Water Resources Research*, 4, 737–747.

Howa, H.L. and Stanley, D.J., 1991. Plant-rich Holocene sequences in the northern Nile delta plain, Egypt: Petrology, distribution and environment of deposition. *Journal of Coastal Research*, 7, 1077–1096.

Inman, D.L. and Jenkins, S.A., 1984. The Nile littoral cell and man's impact on the coastal zone of the southeastern Mediterranean. *Scripps Institution of Oceanography, Reference Series*, 31, 1–43.

IWACO, Consultants for Ground Water and Environment, 1989. Landsat Thematic Mapper for hydrogeological mapping in Egypt. *Report bcrs 89-28, Final report CO1.7, Development and Management of Groundwater Resources in the Nile Valley and Delta Project*, The Netherlands, 50p.

Kerambrun, P., 1986. Coastal lagoons along the southern Mediterranean coast (Algeria, Egypt, Libya, Morocco, Tunisia): Description and bibliography. *UNESCO Reports in Marine Sciences*, Paris, 34, 184p.

Kulyk, V.A., 1987. Holocene foraminifera of the eastern Nile Delta, Egypt. M.Sc. Thesis, George Washington University, Washington, D.C. 90p.

Lighty, R.G.; Macintyre, I.G., and Stuckenrath, R., 1982. *Acropora palmata* reef framework: A reliable indicator of sea level in the western Atlantic for the past 10,000 years. *Coral Reefs*, 1, 125–130.

Maldonado, A. and Stanley, D.J., 1979. Depositional patterns and late Quaternary evolution of two Mediterranean submarine fans: A comparison. *Marine Geology*, 31, 215–250.

MEDIBA (Mediterranean Basin Program), 1992. *Nile Delta Project Data-base Listings.* Records, U.S. National Museum of Natural History, Smithsonian, Washington, D.C.

Mörner, N.A., 1976. Eustatic changes during the last 8000 years in view of radiocarbon calibration and information from the Kattegutt region and other northwestern coastal areas. *Paleogeography, Paleoclimatology, Paleoecology*, 19, 63–85.

Nafas, M.G.; Fanos, A.M., and Elganainy, M.A., 1991. Characteristics of waves off the Mediterranean coast of Egypt. *Journal of Coastal Research*, 7(3), 665–676.

Neev, D.; Greenfield, L., and Hall, J.K., 1985. Slice tectonics in the eastern Mediterranean basin. *In:* Stanley, D.J. and Wezel F.-C. (eds.), *Geological Evolution of the Mediterranean Basin.* New York: Springer-Verlag, pp. 249–269.

Nummedal, D. and Swift, D.J.P., 1987. Transgressive stratigraphy at sequence-bounding unconformities: some principles derived from Holocene and Cretaceous examples. *In:* Nummedal, D.; Pilkey, O.H., and Howard, J.D. (eds.), *Sea-Level Fluctuation and Coastal Evolution.* Society of Economic Paleontologists and Mineralogists, Special Publication 41, pp. 241–260.

Paulissen, E. and Vermeersch, P.M., 1989. Behaviour of large allogenous river systems: the example of the Saharan river Nile during late Quaternary. *Bulletin de la Société Géologique de France*, 8(5), 73–83.

Petit-Maire, N., 1989. Interglacial environments in presently hyperarid Sahara: Paleoclimatic implications. *In:* Leinen, M. and Sarnthein, N. (eds.), *Paleoclimatology and Paleometeorology: Modern and Past Patterns of Global Atmospheric Transport*, Boston, Massachusetts: Kluwar, pp. 637–661.

Pimmel, A. and Stanley, D.J., 1989. Verdinized fecal pellets as indicators of prodelta and delta-front deposits in the Nile delta, Egypt. *Marine Geology*, 86, 339–347.

Pugliese, N. and Stanley, D.J., 1991. Ostracods, depositional environments and Late Quaternary evolution of the eastern Nile delta, Egypt. *Il Quaternario* (in press).

Quelennec, R.E., 1977. Eastern Mediterranean stormy weather and wave climatology off the Nile delta. *In: Proceedings of Seminar on Nile Delta Shore Processes (with Emphasis on Hydrodynamical Factors)*, UNDP/UNESCO, Alexandria, Egypt, pp. 81–115.

© 2001 INIST CNRS. Tous droits de propriété intellectuelle réservés. Reproduction, représentation et diffusion interdites. Loi du 01/07/92. Articles 5, 6 et 7 des CGV.

REINECK, H.E. and SINGH, I.B., 1980. *Depositional Sedimentary Environments.* Berlin: Springer-Verlag, 549p.

RIEHL, H. and MEITIN, J., 1979. Discharge of the Nile River: A barometer of short-period climatic variations. *Science,* 206, 1178–1179.

RITTMANN, A. and NAKHLA, F.M., 1958. Contributions to the study of the Egyptian black sands. *Egyptian Journal of Chemistry,* 1, 125–135.

RIZZINI, A.; VEZZANI, F.; COCOCCETTA, V., and MILAD, G., 1978. Stratigraphy and sedimentation of a Neogene-Quaternary section in the Nile Delta area (A.R.E.). *Marine Geology,* 27, 327–348.

ROSS, D.A. and UCHUPI, E., 1977. Structure and sedimentary history of southeastern Mediterranean Sea–Nile Cone area. *Bulletin of the American Association of Petroleum Geologists,* 61, 872–902.

SAAD, M.A.H. and EZZAT, A., 1972. The bottom of lake Idku, Egypt. *Rapport de la Commission Internationale pour l'Exploration de la Mer Méditerranée,* 21.3, pp. 129–132.

SAID, R., 1981. *The Geological Evolution of the River Nile.* New York: Springer-Verlag, 151p.

SESTINI, G., 1989. Nile delta: A review of depositional environments and geological history. *In:* WHATELEY, M.G.K. and PICKERING, K.T. (eds.), *Deltas: Sites and Traps for Fossil Fuels.* Geological Society of London, Special Publication 41, pp. 99–127.

SHUKRI, N.M., 1950. The mineralogy of some Nile sediments. *Quaternary Journal of the Geological Society, London,* 105, 511–534.

SMITH, S.E. and ABDEL-KADER, A., 1988. Coastal erosion along the Egyptian delta. *Journal of Coastal Research,* 4, 244–255.

STANLEY, D.J., 1978. Ionian Sea sapropel distribution and late Quaternary paleoceanography in the eastern Medditteranean. *Nature,* 274, 149–152.

STANLEY, D.J., 1988. Subsidence in the northeastern Nile delta: Rapid rates, possible causes and consequences. *Science,* 240, 497–500.

STANLEY, D.J., 1990. Recent subsidence and northeast tilting of the Nile delta, Egypt. *Marine Geology,* 94, 147–154.

STANLEY, D.J. and CHEN, Z., 1991. Distinguishing sand facies in the Nile delta, Egypt, by stained grain and compositional component analysis. *Journal of Coastal Research,* 7, 363–377.

STANLEY, D.J. and HAMZA, F.H., 1992. Terrigenous-carbonate sediment interface (Late Quaternary) along the northwestern margin of the Nile Delta, Egypt. *Journal of Coastal Research,* 8(1), 153–171.

STANLEY, D.J.; WARNE, A.G.; DAVIS, H.R.; BERNASCONI, M.P., and CHEN, Z., 1992. Late Quaternary evolution of the North-Central Nile Delta between Manzala and Burullus Lagoons, Egypt. *National Geographic Society Research & Exploration,* 8, 22–51.

SUMMERHAYES, C.P.; SESTINI, G.; MISDORP, R., and MARKS, N., 1978. Nile delta: Nature and evolution of continental shelf sediments. *Marine Geology,* 27, 43–65.

SWIFT, D.J.P., 1968. Coastal erosion and transgressive stratigraphy. *Journal of Geology,* 76, 444–456.

TITUS, J.G. (ed)., 1986. *Effects of Changes in Stratospheric Ozone and Climate change, vol. 4: Sea Level Rise.* Washington: U.S. Environmental Protection Agency, pp. 165–189.

TOUSSOUN, O., 1922. Mémoires sur les anciennes branches du Nil. Epoque Ancienne. *Mémoire de 'Institut d'Egypte,* 4, 212p.

TOUSSOUN, O., 1934. Les ruines sous-marines de la Baie d'Aboukir. *Bulletin de la Société Royale d'Archéologie, Alexandrie,* 29, 342–352.

UNDP/UNESCO. 1976. *Proceedings of Seminar on Nile Delta Sedimentology.* UNDP, Alexandria, 257p.

UNDP/UNESCO. 1977. *Proceedings of Seminar on Nile Delta Shore Processes.* UNDP, Alexandria, 624p.

UNDP/UNESCO. 1978. *Coastal Protection studies. Project Findings and Recommendations.* UNDP/EGY/73/063, Paris, 483p.

U.S. DEFENSE MAPPING AGENCY, 1977. Sheets 5387.1, 5387.2, 5387.3, 5387.4, 5388.2, Series P773, Edition 3-DMA (scale—1:50,000).

U.S. DEFENSE MAPPING AGENCY, 1981. Sheet NH 36-1, Series 1501, Edition 3 (scale—1:250,000).

WARNE, A.G. and STANLEY, D.J., 1991. Expanding dune and salt flats and diminishing lagoons in the Nile delta: Global warming-aridification, other natural processes, or man? *Geological Society of America Abstracts with Programs,* 23, 355.

WATERBURY, J., 1979. *Hydropolitics of the Nile Valley.* Syracuse, New York: Syracuse University Press, 301p.

WEIR, A.H.; ORMEROD, E.C., and EL MANSEY, I.M.I., 1975. Clay mineralogy of sediments of the western Nile delta. *Clay Minerals,* 10, 369–386.

WENDORF, F.; SCHILD, R.; SAID, R.; HAYNES, C.V.; GAUTIER, A., and KOBUSIEWICZ, M., 1976. The prehistory of the Egyptian Sahara. *Science,* 193, 103–113.

WILGUS, C.K.; HASTINGS, B.S.; KENDALL, C.G.ST.C.; POSEMENTIER, H.W.; ROSS, C.A., and VAN WAGONER, J.C. (eds.), 1988. *Sea-Level Changes: An Integrated Approach.* Society of Economic Paleontologists and Mineralogists, Special Publication 42, 306p.

WUNDERLICH, J., 1988a. Investigation on the development of the western Nile delta in Holocene times. *In:* VAN DEN BRINK, E.C.M. (ed.), *The Archaeology of the Nile Delta, Problems and Priorities.* Amsterdam: Netherlands Foundation for Archaeological Research in Egypt, pp. 251–257.

WUNDERLICH, J., 1988b. The natural conditons for pre- and early dynastic settlement in the western Nile delta around Tell El-Farin-Buto. *In:* KRZYZANIAK, L. and KOBUSIEWICZ, M (eds.), *Environmental Change and Human Culture in the Nile Basin and Northeast Africa until 2nd Millenium BC.* Proceedings of the Symposium at Poznan, 1–11. Poznan, Poland: Poznan Archaeological Museum.

ZAGHLOUL, Z.M.; TAHA, A.A.; HEGAB, O., and EL-FAWAL, F., 1977. The Neogene-Quaternary sedimentary basins of the Nile delta. *Egyptian Journal of Geology,* 21, 1–19.

© 2001 INIST CNRS. Tous droits de propriété intellectuelle réservés. Reproduction, représentation et diffusion interdites. Loi du 01/07/92. Articles 5, 6 et 7 des CGV.

□ ZUSAMMENFASSUNG □

Das nordwestliche Nildelta zwischen der Rosetta-Mündung und der Kalkrippe von Abu-Qir wird charakterisiert durch eine konkarve Küstenlinie vor der Idku-Lagunge, ausgedehnte Sandflächen und Dünen. Die spätquartäre Entwicklung dieser Region wird interpretiert vor allen auf der Basis einer petrographischen und Fannen-Analyse von 22 radiokarbondatierten Bohrungen. Die Untergrundstudie ergab dünne holozäne Abschnitte im süd-westlichen Sektor, früher unbekannte marine Buchten-faziez im westlichen Sektor, dicke pflanzenreiche Marschablagerungen im östlichen Sektor, mächtige Nehrungssande im nördlichen und fluviale Sande am Rosettavorsprung. Die Interpretation der Sedimentverteilung im Untergrund und die Paläogeographie berücksichtigt sowohl die Naturfaktoren der Sedimentverteilung (eustatische Meeresspiegelschwankungen, Absinktendenzen, Paläoklima und Transportprozesse) und den Einfluß des Menschen. Das daraus erkennbare Deltabild der letzten 35,000 Jahre wird durch eine Serie von Zeitschnitten in paläographischen Karten dargestellt. Diese Karten berücksichtigen insbesondere die Wanderung der Küstenlinie, die Verlagerung der Hauptabflußkanäle und die Schrumpfung der Lagunen. Jungpleistozäne und früh-holozäne Sequenzen (35,000–7,500 BP) enthalten überwiegend klastiche silikatische alluviale Flachwasserablagerungen. Holozäne Sequenzen seit 7,500 BP umfassen: Deltafront-, marine Buchten-, Lagunen-, Marsch-, und Deltaebenen-Faziez. Die Akkumudationsraten übersteigen lokal 600 cm/1,000 Jahre und sind am größten im sandreichen Rosettavorsprung. Das Untersuchungsgebiet umfaßt—im Gegensatz zum Deltagebiet im Osten—Ablagerungen offener Meeresbuchten und bis 5 m mächtige Torfe und belegt auch eine schwache Auftauchung südlich der Kalkrippe von Abu Qir. Position und Alter früherer Nilmündungsarme wurden erkannt durch die Analyse radiokarbondatierter Bohrungen. Sie umfassen einen großen prähölozänen Kanal, welcher direkt östlich von Abu-Qir in die sog. Abu-Qir-Bay mündet und sich früher wahrscheinlich auf dem Schelf fortsetzte. Während des Holozäns lag der nord-fließende Canopic-Kanal zunächst am Westrand der Idku-Lagune (ca. 6,900–4,000 BP), wanderte dann westwärts der Abu Qir Rippe (4,000–3,000 BP) und bewegte sich wieder ostwärts zu seiner früheren Lage an der Idku-Lagune (3,000–2,500 BP), wo er bis zuletzt verblieb. Es wird angenommen, daß die Erosion des Canopic-Vorsprungs in der gegenwärtig untergetauchten Abu-Qir-Bucht große Mengen Sand für die Bildung von Strandwällen breiten Sandflächen und Küstendünen am nordwestlichen Delta zur Verfügung gestellt hat. Der Bolbitic-Rosetta-Abfluß nach Osten ist ein jüngeres System (ab ca. 2,500 BP), welcher über die längste Phase seiner Geschichte vom Menschen modifiziert wurde. Flache Langunen existierten im Untersuchungsgebiet seit mindestens 5,000 BP, gerieten aber zunehmend unter menschlichen Einfluß. So ist die noch vor 2,000 Jahren existierende Abu-Qir-Lagune inzwischen vollständig verschwunden. Die größere Idku-Lagune hat als Ergebnis von reduziertem Frischwasserzufluß, Landgewinnung und Bewässerungsprojekten inzwischen nur noch 20% ihrer ursprünglichen Größe. Die Studie weist auch auf die Wichtigkeit des Schutzes dieser natürlichen Flächen und ihre Bedeutung für den Menschen im Nildelta hin.—*Dieter Kelletat, Essen, FRG.*

□ RESUMEN □

En Egipto, entre el promontorio Rosetta y Abu Qir, al noroeste del delta del Nilo, se encuentra una costa cóncava con un banco de carbonatos y apoyada sobre la laguna Idkur, la costa de arena es extendida, plana y medanosa. La evolución del Cuaternario Tardío de esta región, ha sido intepretada primariamente sobre la base de análisis petrológico y faunístico de 22 testigos fechados por medio de radiocarbono. El estudio subsuperficial revela, en los ectores sur y oeste, secciones delgadas del Holoceno, facies de la bahía marina previamente no reconocidas en el sector oeste, gruesas capas ricas en vegetales originarias de las marismas en ese sector oeste, grandes barreras de arena de playa en el sector norte, y notables cantidades de arena derivadas del río en el promontorio Rosetta. Las interpretaciones de la distribución de los sedimentos subsuperficiales y la paleo geografía tienen en cuenta factores naturales que determinan la distribución de los sedimentos (nivel del mar eustático, subsidencia, paleoclima y procesos de transporte de sedimentos) y la influencia humana. La evolución de la configuración deltaica durante los últimos ~35,000 años se presenta en una serie de mapas temporales con cortes paleogeográficos. Estos mapas resaltan la migración costera, la variación del gran sistema de canales y la contracción de la laguna con el tiempo. Las secuencias del Pleistoceno Tardío y los inicios del Holoceno (~35,000 a 7,500 A.P.) incluyen depósitos aluvionales y silicoclásticos marinos poco profundos. Las secuencias del Holoceno (desde ~7,500 años A.P.) incluyen el frente deltaico, la bahía marina, la laguna, las marismas y las facies de la planicie deltaica. En el promontorio Rosetta se encuentra la zona más rica en arenas, con una tasa de acumulación que excede localmente los 600 cm/1,000 años. El área estudiada, en contraste con la región este del delta, comprende los depósitos de la bahía marítima abierta y un importante espesor de turba (a 5 m), y registra alguna emergencia en el área sur del banco de Abu Qir. Las posiciones y edades de los primeros y mayores tributarios de los canales del Nilo de la región, se han evidenciado por medio del análisis de los testigos fechados con radiocarbono. Estos incluyen un gran canal pre-Holoceno el cual se extiende hasta el este del banco Abu Qir, a la que hoy es bahía de Abu Qir y, quizás posteriormente en la plataforma continental egipcia. Durante el Holoceno el canal Canopic, fluyendo hacia el norte, se hallaba situado a lo largo del margen oeste de la laguna Idku (~6,900–4,000 años A.P.), migrando entonces hacia el oeste hacia la región este del banco Abu Qir (4,000–3,000 años A.P.) y variando hacia el este a su primera posición a lo largo del margen oeste de la lagina Idku (~3,000–2,500 años A.P.), donde ha permanecido hasta la actualidad. Se ha postulado que la erosión del promontorio Canopic se halla actualmente sumergida al oeste de la bahía Abu Qir dando un aumento de grandes volumenes de arena los cuales formaron los bancos costeros, los amplios canales y los médanos a lo largo del noroeste del delta. El tributario Bolbitic-Rosetta, del este, es un sistema más joven (desde ~2,500 años A.P.), que durante la mayor parte de esta historia, ha sido modificado por el hombre. Lagunas poco profundas han prevalecido en el área estudiada, al menos desde aproximadamente 5,000 años A.P., y han estado con una creciente influencia humana. La laguna de Abu Qir, que existió hace 200 años, ha desaparecido por completo. La laguna Idku es más grande pero posee sólo un 70% de su dimensión original, como una función de reducido flujo de agua dulce hacia la costa y de los proyectos de riego y de la demanda de tierras. Estos estudios hacen un llamado de atención a la necesidad de proteger estos habitats naturales en el delta del Nilo, los cuales son vitales para el hombre.—*Néstor W. Lanfredi, CIC-UNLP, La Plata, Argentina.*

□ RÉSUMÉ □

Le NW du delta du Nil entre le promontoire de Rosette et le cordon carnonaté d'Abu Qir est caractérisé par sa côte concave donnant sur la lagune d'Idku et par les étendues de sables littoraux et dunaires. Les analyses pétrologiques et faunistiques de 22 sondages datés au radiocarbone permettent d'interpréter l'évolution de la fin du Quaternaire. La subsurface révèle: de minces sections holocènes dans les secteurs Ouest et Sud; des faciès de baie marine qui n'avaient pas encore été reconnus dans le secteur Ouest; d'épaisses couches riches en végétaux d'origine marécageuse dans le secteur Est; une épaisse plage barrière de sable dans le secteur Nord et des sables d'origine fluviatile au promontoire de Rosette. L'interprétation de la distribution du sédiment près de la surface et la paléogéographie tiennent compte des facteurs naturels déterminant la distribution des sédiments (variations eustatiques du niveau de la mer, subsidence, paléoclimats, processus de transport sédimentaire) et de l'impact de l'homme. L'évolution de la configuration de ce delta au cours de 35,000 dernières années est montrée par une série chronologique de cartes paléogéographiques. Ces cartes montrent la migration du rivage, la translation des principaux chenaux et le rétrécissement des lagunes avec le temps. Les séquences fin Pleistocène, début Holocène (35,000–7,500 ans B.P.) comprennent surtout des dépôts aluviaux et des phases silicatées de mer peu profonde. Les séquences holocènes (après 7,500 B.P.) montrent des faciès de front deltaïque, de baie marine, lagune, marais et plaine deltaïque. L'accumulation est plus forte vers le promontoire de Rosette, riche en sables et excède localement 600 cm/1,000 ans. Contrastant avec la zone Est du delta, la région étudiée comprend des dépôts marins de baie, et des tourbes épaisses (jusqu'à 5 m). On y enregistre un exhaussement dans le zone située au Sud du cordon de Abu Qir. L'analyse des sondages datés au radiocarbone révèle les positions et les âges des principaux distributaires du Nil. Un vaste chenal pré Holocène s'étendait juste à l'Est du cordon d'Abu Qir jusqu'à ce qui est de nos jours la baie d'Abu Qir et, peut être plus loins sur le plateau continental egyptien. Au cours de l'Holocène, la branche canopique s'écoulant vers le Nord était tout d'abord positionnée le long du bord ouest de la lagune d'Idju (6,900 à 4,000 ans B.P.), puis migrait vers l'ouest presque jusqu'à l'Est du cordon d'Abu Qir (4,000 à 3,000 ans B.P.), ensuite se redéplacait vers l'Est pour rejoindre sa position antérieure le long de la lagune d'Diku (3,000 à 2,500 ans B.P.) position où il s'est maintenu jusqu'à une période récente. On formule l'hypothèse que l'érosion du promontoire canopique actuellement submergé dans l'Ouest de la baie d'Abu Qir ont fourni d'importants volumes de sables qui ont alimenté les cordons littoraux, les larges plaines sableuses et les dunes littorales du Nord Ouest du delta. La branche Bolbitique-Rosette à l'Est, est un système plus jeune (postérieur à 2,500 ans B.P.) qui, durant toute son histoire, a été modifié par l'homme. Les lagunes de faible profondeur prévalent dans la zone étudiée au moins depuis 5,000 ans B.P.; elles ont été de manière croissante soumises à l'influence humaine. La lagune d'Abu Qir, qui existait encore il y a 200 ans, a complèmement disparu. La lagune d'Idku est 5 fois plus petite que sa taille d'origine, est fonction de la réduction du débit d'eau douce, des travaux d'assainissement et des projets d'irrigation. Cette étude appelle l'attention sur la nécessité de protéger ces habitats naturels qui sont vitaux pour l'homme du delta du Nil.—*Catherine Bousquet-Bressolier, Géomorphologie E P H E., Montrouge, France.*